

## Review: Poly(vinyl alcohol) Functionalizations and Applications

Saad Moulay

**To cite this article:** Saad Moulay (2015) Review: Poly(vinyl alcohol) Functionalizations and Applications, Polymer-Plastics Technology and Engineering, 54:12, 1289-1319, DOI: [10.1080/03602559.2015.1021487](https://doi.org/10.1080/03602559.2015.1021487)

**To link to this article:** <http://dx.doi.org/10.1080/03602559.2015.1021487>



Accepted author version posted online: 28 Jul 2015.  
Published online: 28 Jul 2015.



Submit your article to this journal [↗](#)



Article views: 371



View related articles [↗](#)



View Crossmark data [↗](#)



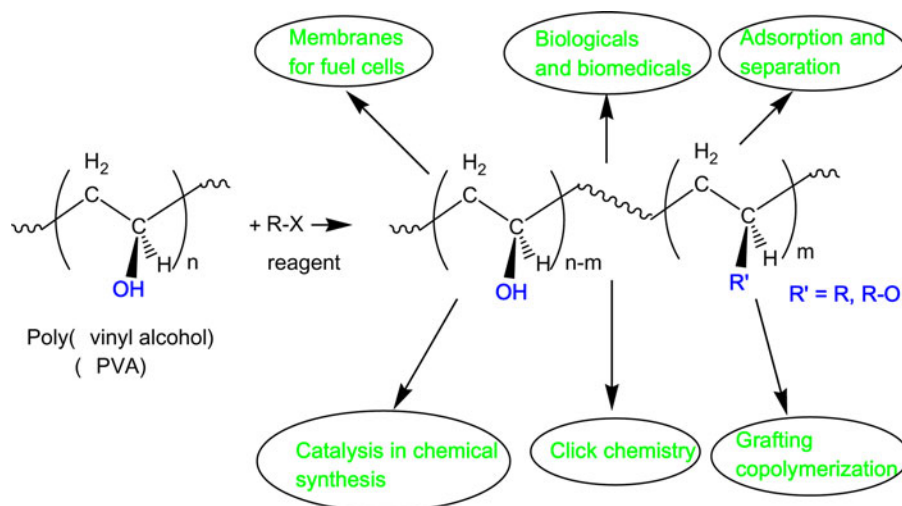
Citing articles: 3 View citing articles [↗](#)

# Review: Poly(vinyl alcohol) Functionalizations and Applications

Saad Moulay

Faculté de Technologie, Laboratoire de Chimie-Physique Moléculaire et Macromoléculaire,  
 Département de Chimie Industrielle, Université Saâd Dahlab de Blida, Blida, Algeria

## GRAPHICAL ABSTRACT



Functionalizations of poly(vinyl alcohol) congruent with the desired applications are discussed in this article. The chemical modifications of poly(vinyl alcohol) with different molecular weights and hydrolysis degrees via conventional chemistries, namely esterification, carbamation, and etherification, and via the modern ones such as click chemistry, led to finished materials with a wide range of applications and uses: membrane fuel cells, biologicals and biomedical, adsorption of heavy metals and other contaminants, molecular sensing or chemosensor for detection of some useful molecules or toxic ones, separation of mixtures, and catalysis in organic and inorganic syntheses. Different forms of the duly modified poly(vinyl alcohol)s were used in such applications, including hydrogels, films, membranes, and nanoparticles. The incorporated modifying agents onto poly(vinyl alcohol) matrixes brought some changes that were in tune with the projected applications. These modifying agents were not confined to molecular compounds but also to macromolecular ones which are graphene, hyaluronic acid,  $\beta$ -cyclodextrin, polystyrene, poly(4-vinylpyridine), and poly(L-lactic acid).

**Keywords** Adsorption; Biomedical; Click chemistry; Fuel cell; Functionalization; Hydrogels; Poly(vinyl alcohol)

## INTRODUCTION

Organic polymers are valuably versatile materials for a great deal of uses and applications. For diverse goals, polymers have

been used either as homopolymers, blends of homopolymers, copolymers, or as chemically modified homo- or copolymers. Nowadays, nearly all industries resort to the use of polymeric materials, in one way or another, insofar their intrinsic properties would be sought for. As known, such properties are partly contingent to the chemical featuring of the polymer, i.e., the chemical binding nature, the organic functional groups, the way these functional groups are linked and the way they are spatially disposed (tacticity)<sup>[1]</sup>. To cite but a few, spellbound and modern applications of polymers encompass

Address correspondence to Saad Moulay, Faculté de Technologie, Laboratoire de Chimie-Physique Moléculaire et Macromoléculaire, Département de Chimie Industrielle, Université Saâd Dahlab de Blida, B.P. 270, Route de Soumâa, 09000 Blida, Algeria, E-mail: [polymchemlab@hotmail.com](mailto:polymchemlab@hotmail.com); [saadmoulay@univ-blida.dz](mailto:saadmoulay@univ-blida.dz)

Color versions of one or more of the figures in the article can be found online at <http://www.tandfonline.com/lpte>.

sensors/biosensors/actuators<sup>[2,3]</sup>, drug delivery<sup>[4]</sup>, sutureless wound closure<sup>[5]</sup>, and photovoltaics<sup>[6,7]</sup>. Mostly, the moieties that secure the properties for such applications are chemical organic/organometallic groups either embedded or covalently anchored onto polymer matrixes, their branches/arms, or their ends. To this end, the latter alternative, that is the covalent attachment, is considered the best route as the affixed group would be an integral part of the polymer. Such finished materials can be achieved by conventional chemical reactions, involving the virgin polymer and the modifying molecule. One of the requirements for the success of such functionalization is the chemical reactivity of the polymer through the existing functional groups. There has been an escalating interest in functionalized polymers as supports, reagents, and catalysts immobilizing<sup>[8,9]</sup>.

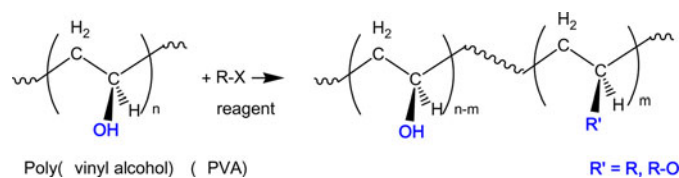
Poly(vinyl alcohol) (PVA), a ubiquitous industrial polymer, is distinguished by its properties and applications<sup>[10–12]</sup>. Starting materials and methods of its synthesis and applications were utterly described<sup>[12]</sup>. A recent synthesis of PVA with controlled molecular weight and high syndiotacticity using reversible addition-fragmentation chain transfer (RAFT) polymerization was reported<sup>[13]</sup>. By its simple structure, PVA has drawn the attention of researchers along its history because of its readiness to chemical reaction via its secondary alcohol functionality<sup>[12]</sup>. In addition, the latter group would account for its solubility in water and organic polar solvents. Its water solubility feature consolidates its superiority as far as environment and green chemistries are nowadays of great concern. The merits of PVA and PVA derivatives lie on their unique biocompatibility, proving their spread uses in biomedical as embolic material<sup>[14]</sup>, orthopedic applications<sup>[15,16]</sup>, and others<sup>[17]</sup>. On the other hand, PVA served as embedding matrix and mat for metallic nanoparticles such as silver nitrate for hydrogen sensor<sup>[18]</sup> and antibacterial activity<sup>[19–21]</sup>, and supporting film for Co/Ag nanoparticles<sup>[22]</sup>. The nanofibers of Fe(III)-complexed PVA were efficient in removing arsenic ions [As(III) and As(V)] from water<sup>[23]</sup>. PVA coating for cobalt ferrite nanoparticles CoFe<sub>2</sub>O<sub>4</sub> nanoparticles (NPs) imparted their toxicity lowering<sup>[24]</sup>.

Accounts of the functionalization of PVA along with their appropriate applications, up to 2008, were reported<sup>[12,25]</sup>. From then, PVA has known an increasing attention as to its applications in its functionalized states, and we deemed important and timely to account for with critical discussion. In this review, it is confined mostly to covalent chemical transformation of PVA, giving rise to soluble materials. Yet, the cross-linking could be invoked if necessary for specific applications, providing that the right and coveted modification has been appropriately made. In some instances, PVA is taken as the functionalizing agent for modifying macromolecules other than linear polymers. Practically, the modification process can occur either on the bulk of PVA (i.e., in solution), or on cross-linked one, or on PVA surface.

Both conventional and novel chemistries have been applied to transform PVA through chemical bonds setting, giving rise

to some novel properties and applications for the virgin polymer. The secondary alcohol functionality is obviously expected to be the preferential reaction site because of its propensity to react under classical chemistry (Eq. 1). The physico-chemical properties and the application extents of the functionalized PVA hinge on the functionalization advance, that is, the substitution degree of hydroxyl groups. Truly noting, the thus-modified PVA is actually a terpolymer consisting of three monomeric units: vinyl acetate (the mother monomeric unit), vinyl alcohol (the hydrolysis resulting monomeric unit), and the vinyl with new functional group (the functionalized vinyl alcohol unit). In some instances and purposely, the newly anchored group can be subjected to further functionalization for specific targets. It is noteworthy to mention that PVA has been viewed as a functionalizing agent for other materials to create, for example, a hydrophilic environment. On the other hand, and because of its reputed properties, not only has PVA been subjected to functionalization but also it has been served as modifying agent to many materials for various purposes. For example, its biocompatibility and biodegradability are highly appreciated when designing biomedical systems. It is worthy of note that, in the last decade, reports on the functionalization all allotropic carbons and derivatives [carbon black, graphite, fullerenes, carbon nanotubes (CNT), graphene, and graphene oxide (GO)] by PVA are distinctly widespread. Also, polymers of different kinds were functionalized with PVA to produce graft copolymers, cross-linked materials and copolymers that look like star copolymers, comb copolymers, and brush copolymers. Functionalization of materials of low molecular weights such as  $\beta$ -cyclodextrin with PVA was accomplished. Hence, in the first place, functionalization of PVA is delineated in parallel with their applications as membrane fuel cells (MFCs), biological and biomedical, adsorption and separation, and catalysis in chemical reactions. In the second place, miscellaneous functionalizations and applications are structured under polymeric grafting, click chemistry, and chemical linkages such as ester, urethane, and ether.

Eq. (1)



## MEMBRANE FUEL CELLS

Membrane fuel cells are evaluated as an alternative technology for the conversion of chemical energy into electrical energy<sup>[26]</sup>. Polymers, including PVA, have been the indispensable mats for developing such ongoing technology. Nafion stands as the standard polymer for MFCs.

Gu et al.<sup>[27]</sup> used PVA (MW = 74–80 kDa) as a cross-linking agent for sulfonated poly(phthalazinone ether sulfone

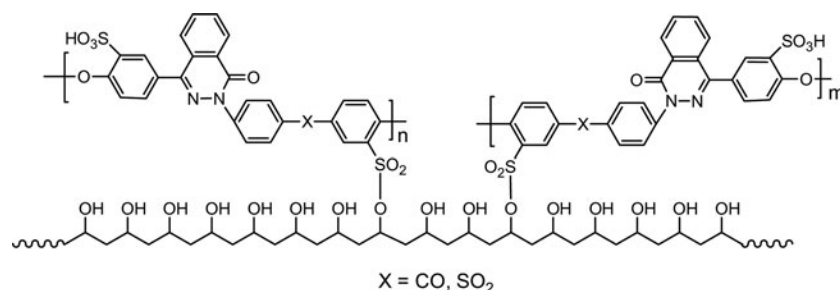


FIG. 1. Structure of S-PPEsk/PVA membranes. Note: S-PPEsk, sulfonated poly(phthalazinone ether sulfone ketone); PVA, poly(vinyl alcohol).

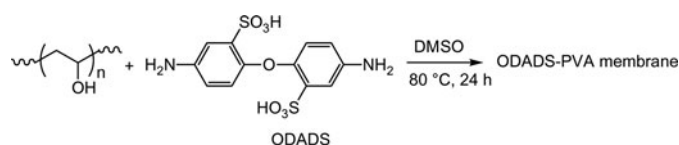
ketone) (S-PPEsk) with degrees of sulfonation  $DS \geq 81\%$ , to produce proton exchange membranes (PEM) (Fig. 1). Cross-linking with 30 wt% PVA took place only at temperatures higher than  $100^\circ\text{C}$ , affording black-colored membranes with defied insolubility. The degree of cross-linking fluctuated between 18 and 38%. The ion-exchange capacity (IEC) of the cross-linked S-PPEsk/PVA membranes was estimated to be  $0.88\text{--}1.85\text{ mmol g}^{-1}$ , depending on the PVA content. Water uptake and swelling ratio of the membrane declined with greater PVA content. At  $80^\circ\text{C}$ , they were measured to be about 110 and 35%, respectively, for 15% PVA, and were 45 and 5% for 35% PVA. Also, the proton conductivity decreased with increasing PVA content, from  $2.00 \times 10^{-2}$  to  $\sim 0.8\text{ S cm}^{-1}$ .

In the aim of elaborating Nafion composite membranes for direct methanol fuel cell (DMFC), the surface of nanofibers (diameter =  $200\text{--}300\text{ nm}$ ) of porous PVA mats made by electrospinning technique were acetalized with 4-formyl-1,3-benzenedisulfonic acid under acidic catalysis at  $60^\circ\text{C}$  for 2 h [28]. The acetalized PVA was cross-linked with glutaraldehyde to be used in the composite formulation. The apparent conductivity of the Nafion/functionalized PVA composite membrane was lower than that of pure Nafion at all temperatures and thicknesses. The IEC of the composite membrane was independent of the membrane thickness and varied from 0.33 to  $0.58\text{ Eq kg}^{-1}$  that of Nafion was almost twice ( $0.93\text{ Eq kg}^{-1}$ ). While the conductivity rose linearly with membrane thickness for Nafion, it increased up to  $\sim 47\text{ }\mu\text{m}$  and decreased beyond for the composite membrane. Tseng et al. [29], however, evaluated the PVA acetalized with 4-formyl-1,3-benzenedisulfonic acid and cross-linked with both 1,3-bis(3-glycidyloxypropyl)tetramethyldisiloxane and 4,4'-oxydiphthalic anhydride as PEMs for DMFC applications. The water uptake, the IEC, and the proton conductivity decreased as the cross-linking density increased from 3 to 50 wt%; water uptake from  $\sim 140$  to  $\sim 50\%$ ; and IEC from  $\sim 2.5$  to  $\sim 1\text{ mEq kg}^{-1}$ . The cross-linking enhanced the oxidative stability of the membrane. A positive temperature effect on the proton conductivity was observed. The proton conductivity of the membrane with 3% cross-linking was measured to be  $0.218\text{ S cm}^{-1}$  at  $70^\circ\text{C}$ , a conductivity higher than that of Nafion 117 ( $0.127\text{ S cm}^{-1}$ ). The methanol permeability was  $\sim 1.25\text{--}1.76 \times 10^{-6}\text{ cm}^2\text{ s}^{-1}$  at  $30^\circ\text{C}$  that for Nafion 117 was  $\sim 2.25\text{--}2.29 \times 10^{-6}\text{ cm}^2\text{ s}^{-1}$ .

The mechanical properties were: tensile strengths of  $10.14\text{--}27.44\text{ MPa}$ , Young's moduli of  $0.52\text{--}0.71\text{ GPa}$ , and elongations at break of  $1.96\text{--}3.89\%$ .

Membranes, conceived by immobilizing 4,4-diaminodiphenylether-2,2-disulfonic acid (ODADS) onto PVA (MW = 72 kDa, Hy = 99.5%), were evaluated in proton exchange for DMFC [30]. It was claimed that ODADS was indeed part of the PVA matrix without indicating how. Yet, we believe that, under the described experimental conditions (Eq. 2), an esterification could have occurred between one of the sulfonic groups and hydroxyl group of PVA. The  $T_g$ s of ODADS-PVA membranes were in the range of  $71\text{--}96^\circ\text{C}$ , and increased with increasing ODADS content; the  $T_g$  of pure PVA was  $85^\circ\text{C}$ . The highest proton conductivity,  $16.53\text{ mS cm}^{-1}$ , was observed for an ODADS content of 20 wt% and at  $30^\circ\text{C}$ , the highest water uptake (98.65%) and methanol permeability ( $7.70 \times 10^{-10}\text{ mol cm}^{-1}\text{ s}^{-1}$ ) were measured for an ODADS content of 10 wt%.

Eq. (2)



Kim and coworkers [31,32] designed nanocomposite membranes for DMFCs by functionalizing CNTs and PVA-appended graphene oxide (PVA-g-GO) with sulfonated PVAs (S-PVA) (Fig. 2a and 2b). The latter S-PVAs were achieved by the treatment of PVA with sodium hydride for 3 h at room temperature, followed by reaction with propane sultone for 3 h at  $80^\circ\text{C}$  (as shown in Eq. 3). The GO nanosheets were esterified with PVA in DMSO in the presence of *N,N*-dicyclohexylcarbodiimide (DCC) and 4-(*N,N*-dimethylamino)pyridine (DMAP) for 3 days at  $50^\circ\text{C}$ . The different membranes containing sulfonic acid groups were cross-linked with glutaraldehyde. The glass transition temperatures of S-PVA were higher ( $80^\circ\text{C}$ ) than that of PVA ( $74^\circ\text{C}$ ), and that of PVA-g-GO was  $79^\circ\text{C}$  due to the restricted mobility of GO sheets. However, the  $T_g$  of the PVA-g-GO/S-PVA membrane increased with increasing PVA-g-GO content, from  $\sim 88$  to

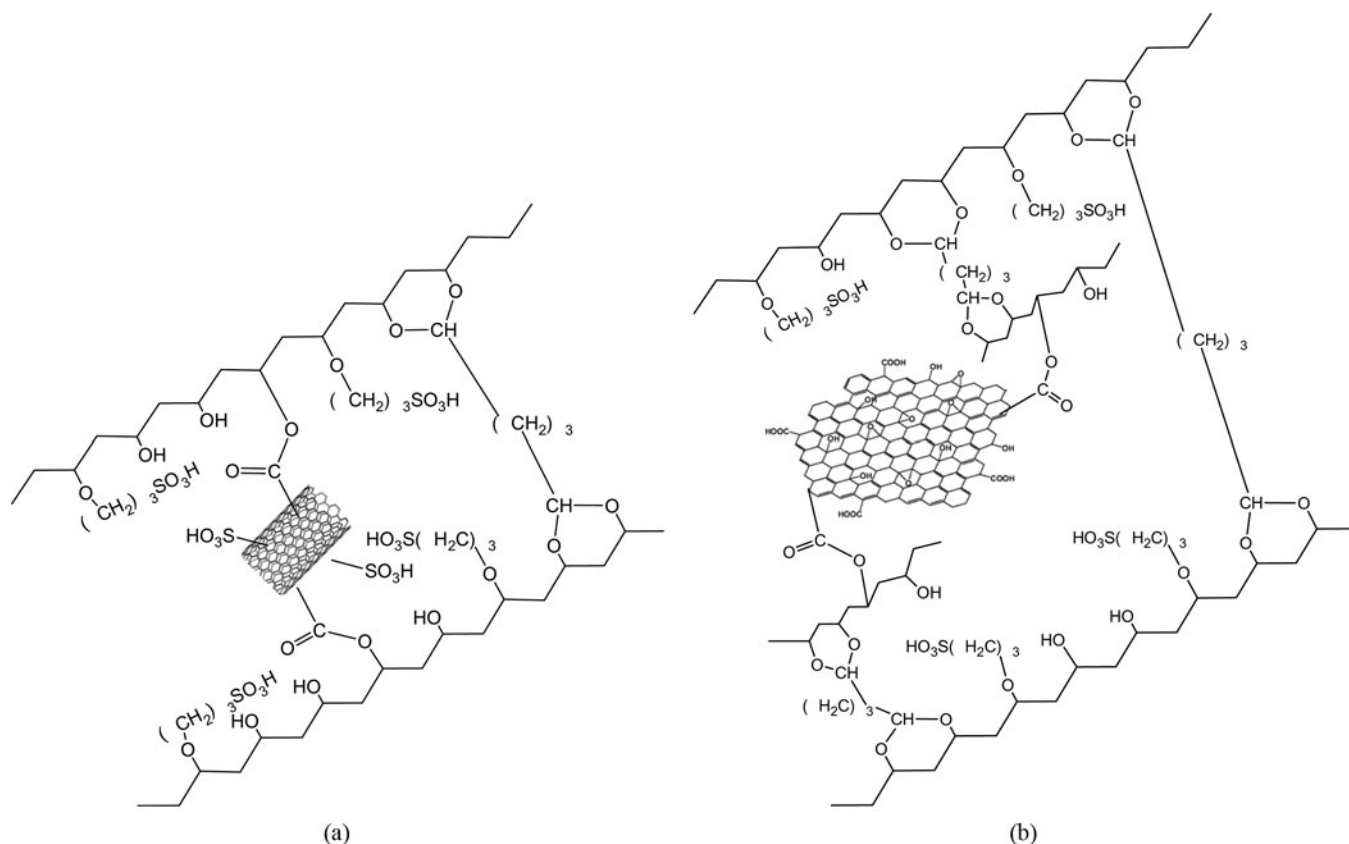


FIG. 2. (a) Sulfonated PVA-g-MWCNT and (b) sulfonated PVA-g-GO. Note: PVA, poly(vinyl alcohol); MWCNT, multi-walled carbon nanotubes; GO, graphene oxide.

$\sim 105^\circ\text{C}$ . The thermal stability, a key factor for PEM cells, of the PVA-g-GO/S-PVA membrane also increased with PVA-g-GO content; in general, the decomposition of the hydroxyl groups of the PVA backbone occurred at  $\sim 150\text{--}200^\circ\text{C}$  and that of the main chain at  $\sim 300\text{--}480^\circ\text{C}$ . The other PEM factors of the PVA-g-GO/S-PVA membrane, IEC, water uptake, proton conductivity, and methanol permeability decreased with increasing PVA-g-GO from 0 to 10 wt% because of the stronger acidity of the sulfonic acid group:  $0.655\text{--}0.545\text{ mEq g}^{-1}$ ,  $154\text{--}49\%$ ,  $0.0206\text{--}0.0097\text{ S cm}^{-1}$ ,  $5.4 \times 10^{-7}$  to  $1.53 \times 10^{-7}\text{ cm}^2\text{ s}^{-1}$ , respectively. The thermal analysis of nanocomposite membrane made from S-PVA and sulfonated multi-walled carbon nanotubes (S-MWCNT) revealed the decomposition of the hydroxyl groups at  $\sim 150\text{--}200^\circ\text{C}$  and another one at  $300\text{--}330^\circ\text{C}$ . The IEC of the S-MWCNT/S-PVA membrane increased ( $0.7\text{--}2.25\text{ mEq g}^{-1}$ ) with increasing S-MWCNT content (0–20 wt%), and the water uptake and methanol uptake decreased from 156.93 to 38.21% and 15.64 to 2.85% at  $25^\circ\text{C}$ , respectively. The highest methanol permeability ( $1.21 \times 10^{-8}\text{ cm}^2\text{ s}^{-1}$ ) was measured for S-MWCNT content of 1 wt% beyond which it decreased, down to  $3.32 \times 10^{-9}\text{ cm}^2\text{ s}^{-1}$ , with increasing S-MWCNT content. The proton conductivity of the S-PVA membrane was in the spectrum of  $0.032\text{--}0.075\text{ S cm}^{-1}$  at  $60^\circ\text{C}$ , and that of the

S-MWCNT/S-PVA membranes increased with increasing S-MWCNT content,  $\sim 0.028$  to  $\sim 0.073\text{ S cm}^{-1}$ .

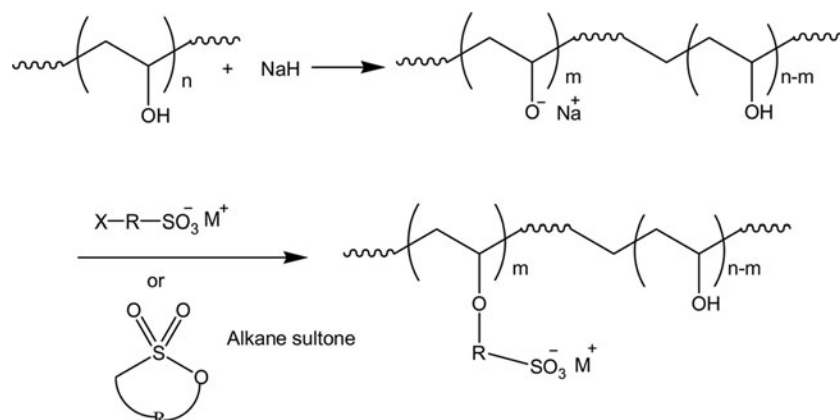
Functionalization of MWCNTs with PVA could be promoted via treatment of the polymer matrix with ozone<sup>[33,34]</sup>; peroxide and hydro peroxide groups would have been formed on PVA matrix. Reaction of the MWCNTs with the ozonized PVA at  $80^\circ\text{C}$  for 3 h afforded PVA-grafted MWCNTs, a 25% of grafting through ether linkage. Spectroscopic analyses, including Fourier transform infrared spectroscopy, X-ray photoelectron spectroscopy (XPS), Raman, and thermal analysis confirmed such grafting. Membranes based on these PVA-grafted MWCNTs and the KOH-doped were evaluated in direct methanol alkaline fuel cells (DMAFC). Water uptake and water diffusion coefficient of PVA-g-MWCNT were  $2.94\text{ g g}^{-1}$  and  $3.09 \times 10^{-7}\text{ cm}^2\text{ s}^{-1}$ , values greater than those for PVA ( $2.81\text{ g g}^{-1}$  and  $2.14 \times 10^{-7}\text{ cm}^2\text{ s}^{-1}$ ), and its methanol permeability was  $2.99 \times 10^{-7}\text{ cm}^2\text{ s}^{-1}$  against  $3.51 \times 10^{-7}\text{ cm}^2\text{ s}^{-1}$ . The ionic conductivity of the PVA-g-MWCNT doped with 6 M KOH at  $60^\circ\text{C}$  was measured as  $11.76 \times 10^{-7}\text{ S cm}^{-1}$  and that of PVA was  $10.88 \times 10^{-7}\text{ S cm}^{-1}$ . The outcome of their performance in DMAFC (2 M methanol fuel in 6 M KOH at  $60^\circ\text{C}$ ) was  $39\text{ MW cm}^{-2}$  in power density and 0.86 V in potential.

In a patent, Goldbach<sup>[35]</sup> reported a series of membrane electrode assembly (MEA) for fuel/electrochemical cells set



by blending fluoropolymers ( $MW = 80\text{--}1000\text{ kDa}$ ) and polyelectrolytes that have no hydrolyzable units. Of these, polyelectrolytes were the S-PVAs as those shown in Eq. (3). These PVA-based polyelectrolytes were generally prepared by reaction of PVA ( $MW = 144\text{ kDa}$ ,  $Hy = 99\%$ ) with sodium hydride acting as a strong base, followed by reaction with haloalkane sulfonate or alkane sultone in anhydrous DMSO at room temperature for 18 h. Sulfopropylated and sulfobutylated could be obtained with a degree of sulfonation ranging between 10 and 100%.

Eq. (3)



Recently, Korean school<sup>[36]</sup> evaluated the cross-linked quaternized PVA (Q-PVA) [see Eq. (22) below] with glutaraldehyde as an ionomer binder, and the MEAs made therefrom for solid alkaline fuel cells. The optimal intrinsic parameters of such As-made MEAs were  $2.3 \times 10^{-3}\text{ S cm}^{-1}$  in ionic conductivity and  $1.2\text{ mEq g}^{-1}$  in IEC. Better performance of MEAs was observed for the one made with 25 wt% ionomer binder, showing a power density of  $172.8\text{ MW cm}^{-2}$  for a current density of  $360\text{--}380\text{ mA cm}^{-2}$  and a cell voltage of about 0.48 V.

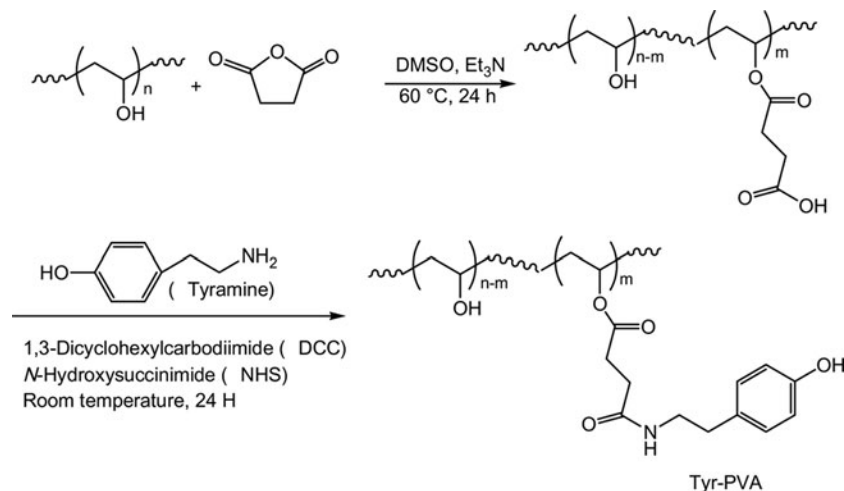
## BIOLOGICAL AND BIOMEDICAL APPLICATIONS

By now, the uses of polymers in biomedical are widespread<sup>[37]</sup> because they offer several advantages that are in tune with their inherent properties, and are relevantly coined “biomaterials”. By far, The mostly used polymers in biological and biomedical are PVA and poly(ethylene glycol) in the form of hydrogels.

Lim et al.<sup>[38]</sup> developed biosynthetic hydrogels that are prone to load tyrosine containing proteins and endowed with biological functions for tissue engineering applications. To this intent, tyramine was grafted through the succinyl groups initially attached to PVA ( $MW = 13\text{--}23\text{ kDa}$ ;  $Hy = 98\%$ ) to

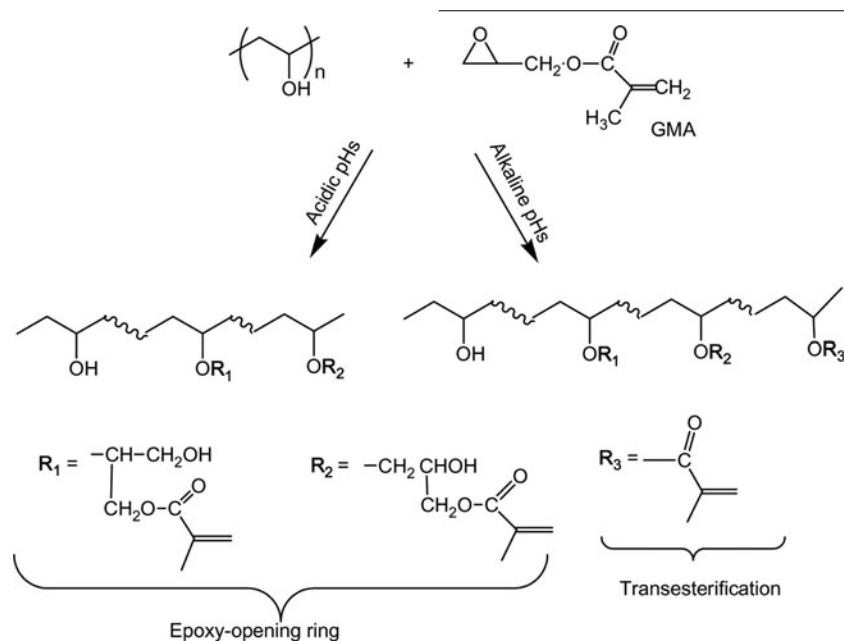
afford Tyr-PVA as depicted in Eq. (4). Hydrogels were prepared by mixing the solutions of Tyr-PVA and gelatin in Dulbecco’s phosphate buffered saline, followed by addition of catalytic amounts of sodium persulfate and tris(2,2-bipyridyl)dichlororuthenium(II) hexahydrate as initiators. All the systems were then irradiated to promote the gel formation. The mechanism by which the gel was formed is the formation of carbon–carbon bonds between phenol groups of the tyrosine of the gelatin and those of Tyr-PVA.

Eq. (4)



A pendant methacrylate group from PVA matrix is conceived through the reaction of the latter polymer with glycidyl methacrylate (GMA). The reaction commonly occurs between the hydroxyl groups of PVA and the epoxy group of GMA when the modification is conducted in organic solvents. Yet, the attachment site is pH-dependent when modification is run in waterborne systems<sup>[39]</sup>; at acidic pHs (3.5), the reaction of GMA with PVA occurs exclusively via epoxy-opening ring, and at alkaline pHs (10.5) it takes place via both transesterification and epoxy-opening ring, the latter being predominant (Eq. 5).

Eq. (5)



Crispim et al.<sup>[40]</sup> grafted methacryloyl groups on PVA (MW = 23.4 kDa) by reaction with GMA in DMSO at 62°C for 6 h, affording 4.63% of substitution degree. Hydrogels from GMA-modified PVA (GMA-PVA) and blends of GMA-PVA/chondroitin sulfate were prepared in the presence of *N,N,N',N'*-tetramethylethylenediamine and sodium persulfate (chondroitin is a sulfated glycosaminoglycan). Hydrogels from the blends showed greater swelling and the swelling degrees of all the formed hydrogels at 25°C for 48 h decreased with increasing degree of substitution. However, mechanical properties of the hydrogels increased with increasing degree of substitution, and those from the blends showed mechanical properties lower than those from GMA-PVA; for degree of substitution of 5%, the elastic modulus was 95 and 126 kPa, respectively. It seems that chondroitin sulfate diminished the rigidity of GMA-PVA. The shear modulus of the GMA-PVA hydrogels oscillated between 23.60 and 42.19 kPa when the degree of

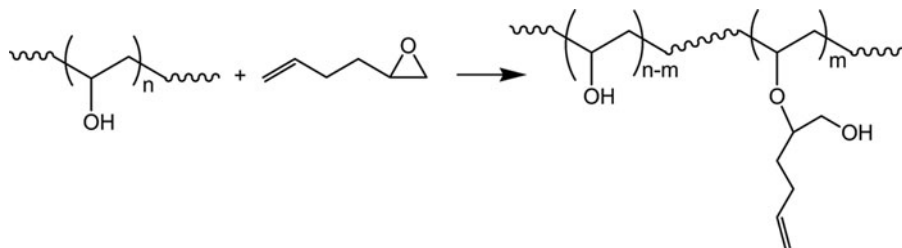
substitution rose from 2.5 to 5.0%. The biological tests of the hydrogels revealed their nontoxicity for cells growth, suggesting their use as safer drug carriers.

Grafting of GMA onto PVA could be induced under UV light using benzophenone as photoinitiator<sup>[41]</sup>. A lipase was covalently immobilized on the GMA-functionalized PVA after activation with carbonyl diimidazole (CDI). The GMA spacer created a hydrophobic environment for interfacial activation of the enzyme. The As-immobilized lipase showed higher enzymatic activity, compared to the free or nonimmobilized one. Elsewhere, nanofibers from PVA functionalized with GMA were achieved by electrospinning in the presence of UV

light<sup>[42]</sup>. Such a functionalization was thought to bring about some improvement of resistance toward solvents. The GMA-functionalized PVA nanofibers were claimed to be potential candidate in tissue engineering.

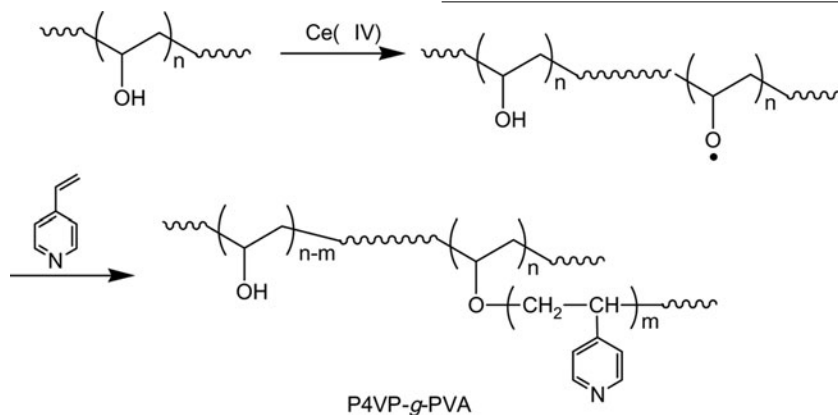
In another reported work, PVA (MW = 85–124 kDa, Hy = 89–99%) underwent functionalization with 2-epoxy-5-hexene by running the reaction in water at a pH of 3 and at 40°C for 48 h (Eq. 6)<sup>[43]</sup>. The glass transition and melting temperatures of the modified PVA were 124–131 and 219–220°C, respectively. The modifying agent 2-epoxy-5-hexene acted as cross-linker in the formation of hydrogels by photopolymerization of the monomers *N*-vinylpyrrolidone, 2-hydroxyethyl acrylate, *N,N*-dimethylacrylamide or acrylic acid, in the presence of 2-hydroxy-1-[4-(2-hydroxyethoxy)phenyl]-2-methyl-1-propanone as photo initiator. The shear storage moduli of the different hydrogels were in the spectrum of 0.4–11.0 kPa. Based on the cytotoxicity tests, the hydrogels were claimed to be advantageous for biomedical applications.

Eq. (6)



Poly(4-vinyl pyridine) (P4VP) was grafted on PVA (DP = 1750, Hy = 95%) by radical polymerization of 4-vinylpyridine (4VP) in the presence of PVA and ceric ammonium sulfate (CAS) as radical initiator<sup>[44,45]</sup> (Eq. 7). The latter initiator takes off protons of the hydroxyl groups to generate radical alkoxy groups to initiate the polymerization. The graft polymerization was conducted in water under nitrogen atmosphere and at 60°C for 4 h. The graft efficiency peaked at ~60% for 4VP concentration of 0.16 mg mol<sup>-1</sup> and 4 m mol L<sup>-1</sup> of CAS, beyond which the graft efficiency dropped. The grafted copolymer P4VP-g-PVA served as coating system in the form of hydrogel layer to polypropylene nonwoven fabric membrane surface to enhance the hydrophilic and antibacterial properties. The contact angles of the As-modified membranes were in the range of 33.3–69.3° that is lower than that of untreated membranes (123°). Both antifouling and antimicrobial properties of the P4VP-g-PVA-modified membranes were improved. The total organic rejection jumped from 39% (for untreated membrane) to 78% for membrane modified with 1.5 wt% P4VP-PVA. No biological cell attachment was observed with membranes modified with P4VP-PVA and the quaternized P4VP-g-PVA (quaternization with benzyl bromide), hinting at the greater antimicrobial activity.

Eq. (7)



Blum and Ovaert<sup>[46,47]</sup> fashioned hydrogel-based lubricants with low boundary friction properties, for a perspective use

as artificial articular cartilage. This was realized by setting hydrogels using from PVA functionalized with a fatty alkyl chain, lauroyl (C<sub>11</sub>H<sub>23</sub>CO-) and stearyl (C<sub>17</sub>H<sub>35</sub>CO-) ones. Functionalization of PVA (MW = 188 kDa, Hy = 99%) proceeded with lauryl/stearyl chloride either in 1-methyl 2-pyrrolidone or DMSO at 50°C for 24 h. The friction test revealed that the lauroylated PVA-based hydrogels had friction coefficients  $\mu$  lower than those for nonfunctionalized PVA-based hydrogels, and they decreased with increasing the lauroyl content, up to 70% decrease of  $\mu$  was observed. However, the stearyl group showed a higher friction test, indicating that there must be a threshold in the fatty alkyl chain for lubrication purposes.

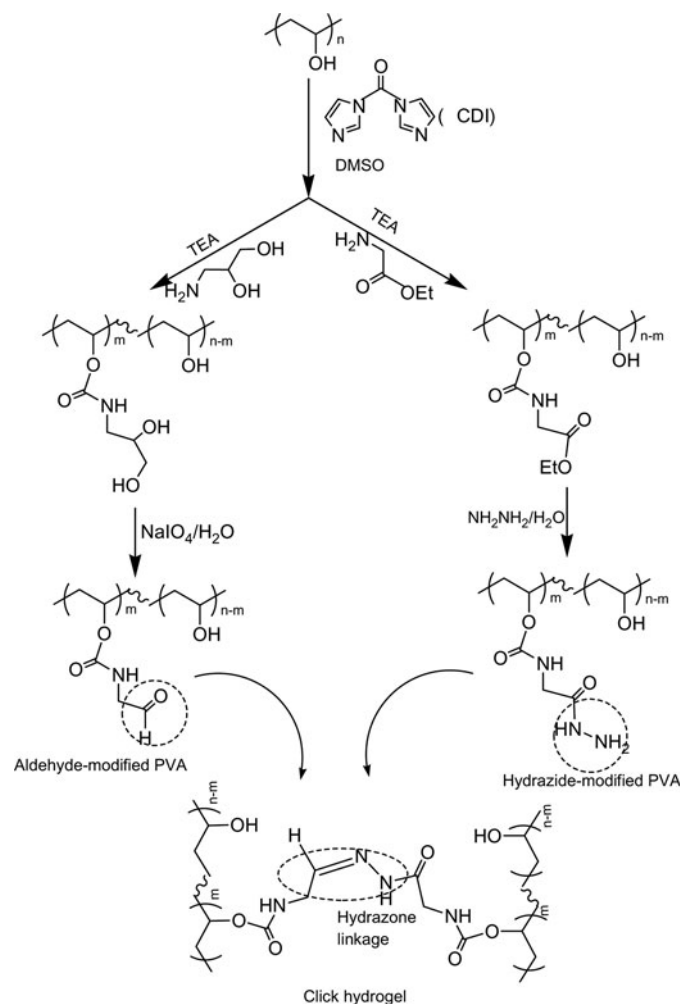
Carbamate linkage to PVA matrix can be set indirectly by exploiting the use of CDI, a coupling agent, and an amine. The CDI has the proneness to react with hydroxyl groups, giving rise to an intermediate that can easily react with amine. Such chemistry was applied by Ossipov and Hilborn<sup>[48]</sup> for the bioconjugation of PVA. This strategy was also used by Alves et al.<sup>[49]</sup> to realize PVA hydrogels that can be cross-linked through hydrazone functions, hydrogels that were tested for their cytotoxicity. The cross-linking via hydrazone functionality was achieved through the click reaction between aldehyde-modified PVA and hydrazide-modified PVA as shown in

Eq. (8). The two functionalized PVAs (MW = 12–23 kDa, Hy = 98%) were obtained as traced, and the degree of



functionalization was confined to 5–10 groups per PVA chain for ensuing hydrogels. The mechanism of the reaction can be found in the review paper by Montalbetti and Falque<sup>[50]</sup>. The As-prepared hydrogels were stable toward hydrolysis for as long as four months, indicating the feature of the hydrazone group as means of cross-linkage.

Eq. (8)

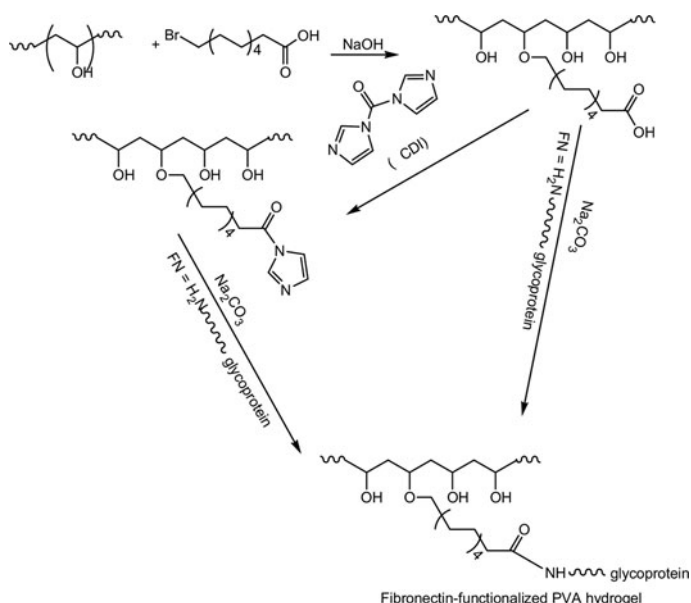


Rafat et al.<sup>[51]</sup> methacrylated PVA (MW = 13–23 kDa, Hy = 88%) to yield MA-PVA as shown in Eq. (20) (see below<sup>[99]</sup>), followed by amination with 4-aminobutylaldehyde diethyl acetal for making hydrogels destined for cell adhesion molecules. The optimal modification extents obtained were ~3.40 mol% of methacrylation and 4.60 mol% of amination. Hydrogels were made by irradiation of the aqueous solutions of MA-PVA and its aminated product in the presence of photo initiator by UV light ( $\lambda = 365$  nm) for 90 s; the cross-linking in the hydrogel was due to the formation of poly(methyl methacrylate). Young's moduli of the hydrogels fluctuated between 130 and 720 kPa and was found to increase with increasing methacrylation extent. Swelling capacity rose with increasing

methacrylation. The thus-made hydrogels demonstrated a higher potency in the adhesion of leukocyte–endothelial cell.

Fibronectin (FN), a glycoprotein, was affixed onto the physically hydrogelled PVA (MW = 146–186 kDa, Hy > 99 %) through an ether linkage by means of reaction with 2-bromodecanoic acid in alkaline conditions, either via *N*-acylimidazole through CDI protocol or not, as depicted in Eq. (9)<sup>[52]</sup>. The obtained FN-grafted-PVA hydrogels, conceived as hydrogel–tissue hybrid materials, were stiffer than the pure PVA hydrogels; at 65% strain, the elastic modulus was 1.60 MPa against 1.02 MPa that is a 57% increase. And, at physiological strain (30%), the elastic modulus was interestingly not too far from that of native tissue, 0.5 MPa against 0.2 MPa. Also, the FN-g-PVA hydrogels showed higher relaxation stress when compared with the PVA control, suggesting that they could recover as native tissue within a cardiac cycle.

Eq. (9)

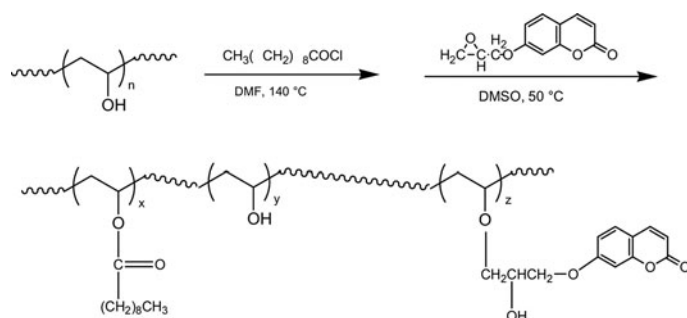


Cross-linking or copolymerization of PVA and  $\beta$ -cyclodextrin (CD) was commonly achieved by means of epichlorohydrin as cross-linker, giving rise to PVA/ $\beta$ -CD hydrogels<sup>[53,54]</sup>. These hydrogels were evaluated as drug carriers. In the report of Sun et al.<sup>[53]</sup>, the PVA- $\beta$ -CD materials could contain up to 73 mol of  $\beta$ -CD per 1000 mol of vinyl alcohol units in PVA matrix. The crystallinity of the PVA- $\beta$ -CD polymers increased with epichlorohydrin concentration. Aspirin, 3-hydroxy-2-naphthoic acid, phenylpropionic acid, and naphthylamine were loaded into the cavities of  $\beta$ -cyclodextrin of the hydrogels and the study of their fluorescein isothiocyanate (FITC)-dextran corresponding release was undertaken. The swelling degree of the loaded hydrogels and their release of phenylpropionic acid and naphthylamine were

pH sensitive; a swelling degree of up to  $\sim 1100\%$  and a FITC-dextran release of up to 40% were measured.

Lee and Kim<sup>[55]</sup> developed a modified PVA–coumarin conjugates for making photoresponsive hydrogels and photoreponsive monoolein cubic phases. To realize the latter system, PVA (MW = 9–10 kDa) was subjected to the reaction with decanoyl chloride in DMF at 140°C for 2 min, followed by reaction with epoxypropylcoumarin (EPC) in DMSO at 50°C for two days as traced in Eq. (10). The resulting decanoyl–PVA–EPC (DC–PVA–EPC) conjugates were successfully immobilized in water channels due to the gained hydrophobicity extent, exerting a greater interfacial activity in the monoolein membrane/water interfaces of the water channels; the critical micellar concentration of this conjugate was measured to be 0.005%, assuring an interfacial tension of about 43 dyne cm<sup>−1</sup>. The DC–PVA–EPC conjugate group acted as polymeric surfactant. The release extent of FITC-dextran from water channels within monoolein cubic phases with PVA–coumarin conjugate incorporation was about 32 and 25% after 72 h without and with UV irradiation ( $\lambda = 254$  nm) for 3 h, respectively; such irradiation induced the dimerization of the coumarin moieties, ensuing a cross-linking of the DC–PVA–EPC conjugate. The latter conjugate system was used in the building of vesicles with photosensitive liposomes for the release of 5(6)-carboxyfluorescein<sup>[56]</sup>. The release of this fluorescein in 1 h was about 25% for phospholipid/DC–PVA–EPC ratio of 1:0.5 and when UV-irradiated at  $\lambda = 254$  nm, and insignificant when nonirradiated; the irradiation induced the photodimerization of EPC residues. Earlier, Wang et al.<sup>[57]</sup> reported the synthesis of EPC-functionalized PVA with fluorescence features.

Eq. (10)

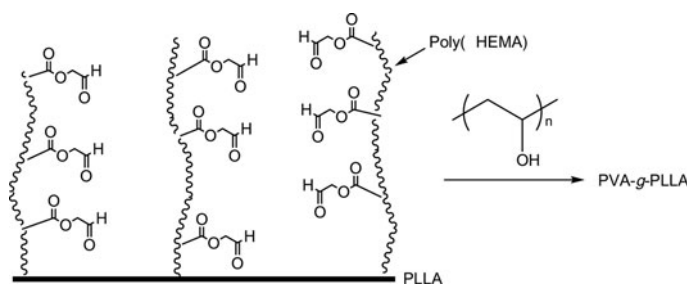


However, hydrogels from PVA–EPC conjugate were made by irradiating its solution in phosphate buffer at  $\lambda = 365$  nm for 1 h, as a result of ensuing cross-linking via cyclic dimerization of EPC residues<sup>[58]</sup>. Release degree of 5(6)-carboxyfluorescein from PVA–EPC hydrogel was found to be higher when the hydrogel was irradiated at  $\lambda = 254$  nm for 5 min, 70% against 53% for nonirradiated hydrogel, in 24 h. This improved release was imputed to a photodimerization of EPC moieties. A further work was devoted to the use of PVA–EPC conjugate in the confection of hollow microcapsules<sup>[59]</sup>.

To this end, the authors conceived a build-up of an oil-in-water (O/W) emulsion composing of PVA–EPC conjugates as an emulsifier and chloroform as an oil component; the emulsion droplets were set by salting-out PVA–EPC with an aqueous 1 M NaCl solution, followed by irradiation-induced cross-linking at  $\lambda = 365$  nm for about 5 min, affording a dimerization extent of 60%. Evaporation of chloroform and dialysis of salt allowed the formation of hollow capsules with a size of about 26  $\mu\text{m}$ . Such a strategy of making photo responsive hollow microcapsules was prospected for drug delivery.

A build-up of PVA-based hydrogels was conceived on poly(L-lactic acid) (PLLA) platform through a multistep sequences involving chemical functionalization<sup>[60]</sup>. An oxygen plasma-treated PLLA film (MW = 117 kDa) was functionalized on surface with poly(2-hydroxyethylmethacrylate), poly(HEMA). Provision of aldehyde functionality on PLLA surface was possible via the oxidation of the grafted poly(HEMA) by pyridinium dichromate, and the subsequent acetalization with PVA (MW = 146–186 kDa, Hy > 99%) gave PVA-immobilized PLLA (Eq. 11). Silver-containing PVA-*g*-PLLA hydrogels were realized by freeze-thaw method. Adhesion of hela cells to the silver-containing PVA-*g*-PLLA hydrogel films was nearly insignificant (0.80%), while that on PLLA surface was almost 80%. These results were not due to the silver nanoparticles, but were accounted in terms of the hydrophilicity of the surface ( $\theta_A = 10^\circ$ ) and the low interfacial tension between the hydrogel surface and the existing environment. However, the good antibacterial activity observed was attributed mainly to the silver nanoparticles.

Eq. (11)



Gelatin was covalently attached to PVA matrix through their methacrylate macromer functionalization, yielding PVA–gelatin hydrogel<sup>[61]</sup>. Gelatin was functionalized with methacrylate macromer by reaction with methacrylic anhydride, and PVA (MW = 13–23 kDa, Hy = 98%) by reaction with 2-isocyanatoethylmethacrylate; the average number of methacrylate functional groups per PVA chain were 7 and 20. Hydrogels were formed by UV light curing of the mixture of PVA-methacrylate macromers and gelatin-methacrylate macromers at different ratios. A decrease in swelling ratio and in mesh size of the hydrogels with increasing methacrylate functional

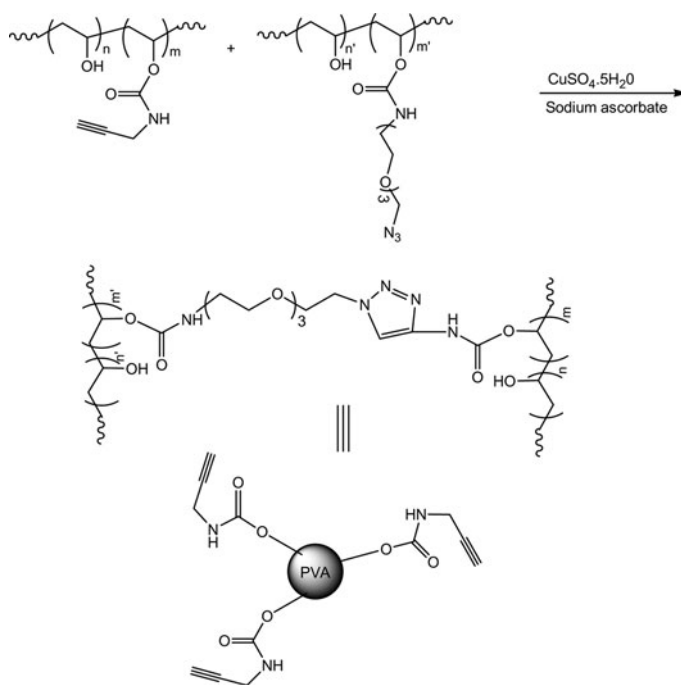
groups was observed. Also, the diffusion of the two proteins studied, bovine serum albumin (BSA) and IgG, dropped. No significant impact of gelatin was detected on these two parameters vis-à-vis to PVA hydrogels. However, PVA-gelatin hydrogels showed far better cell adhesion than PVA hydrogels. These PVA-gelatin hybrids with a content of as low as 1% of gelatin and with a high content of methacrylate macromers were claimed to exhibit promising properties for utilization as cell immunoisolating membrane materials.

To circumvent the drawback of the poor interfacial adhesion when reinforcing PVA hydrogels with ultra-high molecular weight polyethylene (UHMWPE; HDPE with molecular weight of 2000–6000 kDa) fibers for implant surgery purposes, Holloway et al.<sup>[62]</sup> conceived the covalent grafting of PVA on the UHMWPE fiber surface. In this work, the latter surface was treated with oxygen plasma to create hydroxyl and carbonyl groups, followed by the reaction with glutaraldehyde at room temperature for 18 h. The PVA (MW = 89–98 kDa, Hy > 99%) layer was placed via the acetalization reaction with the second aldehyde functionality of the glutaraldehyde. Interfacial shear strength for the thus-made PVA-g-UHMWPE was substantially greater than that for the innate UHMWPE, 228.6 kPa against 11.5 kPa.

Paradossi and coworkers<sup>[63]</sup> conceived microgel particles (diameter of 2  $\mu\text{m}$  and pore size of 3–5 nm) built with PVA (MW = 70 kDa) as a core and hyaluronic acid (HA) as a shell, and studied the biointerface properties of PVA–HA gels. The cores of microgel particles were achieved through click chemistry in an inverse emulsion (Eq. 12) between alkynylated and azidated-PVA chains that were made via CDI technique. The hyaluronic acid shells were constructed also by means of click chemistry between PVA microgel particles having residual alkynyl groups and the azidated HA. Doxorubicin (DOXO), a common cancer therapeutic, was loaded on the PVA–HA microgel particles (Fig. 3), and the PVA–HA/DOXO conjugates were tested on adenocarcinoma colon cells (HT-29 cells). It was claimed that HA had a dual role: targeting the

cancer cells and stabilizing the loaded drug molecules. The DOXO release could be completed within 5 h for a DOXO loading of  $1.95 \times 10^{-2} \text{ mg mg}^{-1}$  of dry coated HA.

Eq. (12)



“Click chemistry” emerged as a straightforward coupling via a cycloaddition between two organic functionalities, namely the Huisgen cycloaddition involving azide and nitrile groups to afford 1,2,3-triazoles. Recently, the application of this chemistry in the supramolecular systems was surveyed<sup>[64]</sup>. It has been exploited in the chemical modification of polymers, mainly PVA. Pyrene and pyrene-bearing molecules were covalently attached to PVA matrix by means of spacers anchored by conventional reactions. Yagci and his coworkers<sup>[65]</sup> designed the attachment of pyrene molecules onto

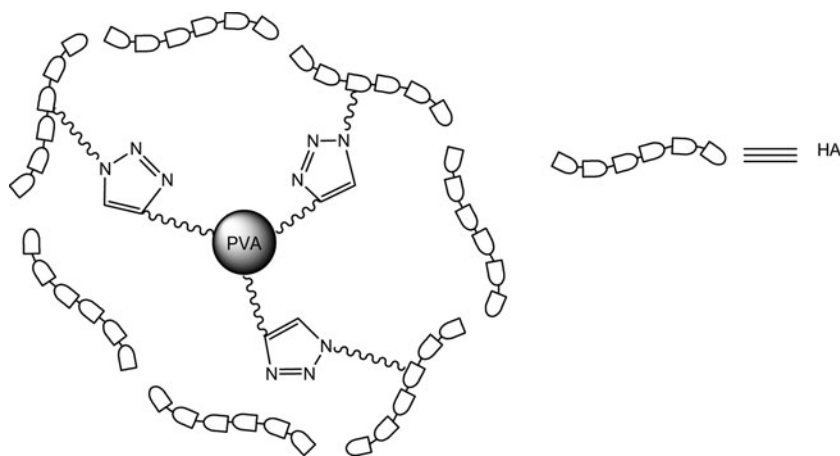
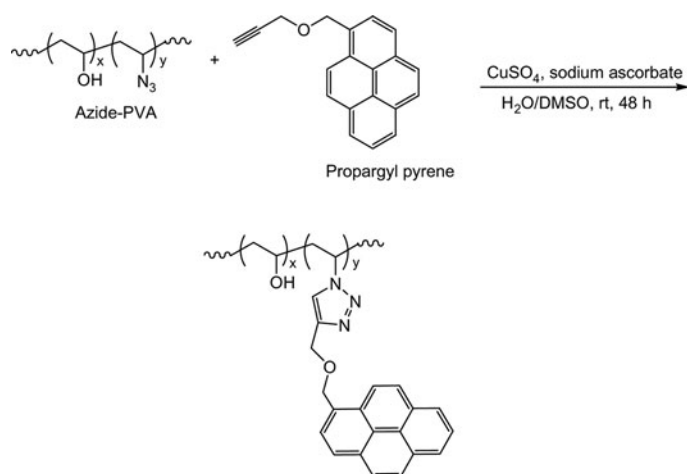


FIG. 3. Microgel particle consisting of PVA and HA linked via click chemistry. Note: PVA, poly(vinyl alcohol); HA, hyaluronic acid.

PVA by an azidation of the tosylated PVA (MW = 63 kDa). The tosylation was realized with tosyl chloride to yield Ts-PVA with 10 wt% Ts. Subsequent azidation was performed using sodium azide in DMF at 60°C, affording N<sub>3</sub>-PVA. Click chemistry was applied to the latter modification with propargyl pyrene as shown in Eq. (13). The success of this chemistry was confirmed by fluorescence emission spectroscopy, the pyrene being photo-active and fluorescence responsive species. The pyrene-functionalized PVA, pyrene-PVA, was soluble in water, DMSO, DMF, and slightly soluble in THF, and was more thermally stable than PVA. This school extended their work by immobilizing the enzyme "glucose oxidase"<sup>[66]</sup> and anti-metadherin<sup>[67]</sup> in pyrene-functionalized PVA after activation of hydroxyl groups with 1-ethyl-3-(3-dimethyl-aminopropyl) carbodiimide hydrochloride, a coupling agent. The enzyme-immobilized modified PVA showed glucose sensing ability using fluorescence technique, and the anti-metadherin pyrene-PVA successfully served as a fluorescent probe for diagnosis of MCF-7 human breast cancer cells.

Eq. (13)

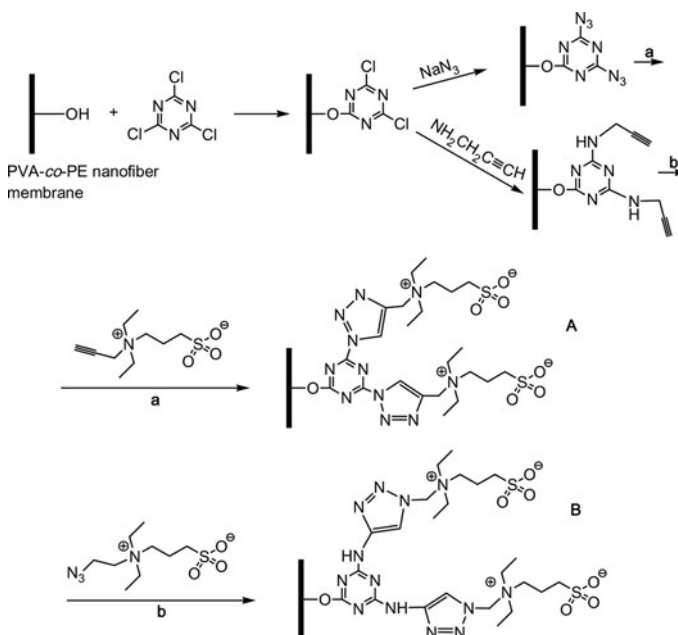


Bai and his coworkers<sup>[68]</sup> designed the making of magnetic microspheres from PVA (DP = 1700) and Fe<sub>3</sub>O<sub>4</sub> magnetite nanoparticles for the enrichment of cell glycoproteins. The alkynylated magnetic microspheres exhibited the potential to react with azide-glycoprotein under click chemistry.

By means of click chemistry, Huang et al.<sup>[69]</sup> were able to affix zwitterionic sulfobetaine on the surfaces of PVA-co-PE nanofiber membranes (Eq. 14). PVA-co-PE membranes were activated with cyanuric chloride, yielding an overall grafting degree of about 41%. The thus-activated membranes were converted into azide- and alkynyl-functionalized PVA-co-PE membranes by reaction with sodium azide, and 2-propynylamine, respectively, and in overall grafting degrees of about 60 and 66%. These functionalized PVA-co-PE membranes underwent click chemistry, respectively, with *N,N'*-diethyl-*N*-propargyl-*N*-(3-sulfopropyl) ammonium and 3-((2-azidoethyl) dimethylammonio) propane-1-sulfonate; the overall grafting

degrees of the zwitterionic sulfobetaine were nearly 68 and 105%. The realized materials A and B displayed an excellent antifouling property with regard to BSA protein.

Eq. (14)



Salicylic acid units could be attached to PVA matrix (MW = 31.6–50 kDa, Hy = 98–99%) through the chloroacetyl spacer for controlled drug delivery<sup>[70]</sup>. Chloroacetylation of PVA was performed with chloroacetyl chloride in dimethylacetamide (DMAc)/LiCl solvent system and in the presence of pyridine, at room temperature for 8 h. A degree of chloroacetylation of as high as 99% could be achieved for an excess of chloroacetyl chloride. Salicylation of chloroacetylated PVA occurred at about the same degree of functionalization (99%), with sodium salicylate in DMSO at 30°C for 5 h. Hydrolysis of the salicylation product gave the PVA-salicylic acid conjugate (Fig. 4a). For PVA-salicylic acid conjugate with 37.8%

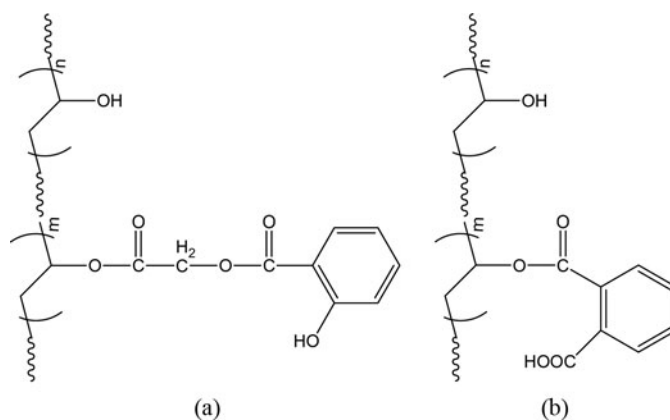


FIG. 4. (a) PVA-salicylic acid conjugate and (b) PVA with aromatic carboxylic group. Note: PVA, poly(vinyl alcohol).



modification degree, about 60% sodium salicylate release was observed after 20 days at a pH of 8.5 and a temperature of 37° C. Under the latter conditions, only 10% of sodium salicylate release was measured for 99% modification degree. Toward the same objective, Cristescu et al.<sup>[71]</sup> esterified PVA with phthalic anhydride (Fig. 4b) in DMF and in the presence of pyridine, to yield PVA with carboxylic functionality. Thin films of the latter functionalized PVA were coated on ibuprofen tablets by deposition via by matrix-assisted pulsed laser evaporation. The coating was revealed to be stable for 9 and 14 min in acidic and alkaline media, respectively, after which the dissolution rate increased; it is expected a gastro-resistance to the tablets within these stability times.

By properly adjusting the [CHO]/[OH] molar ratio of glutaraldehyde and PVA, acetalized PVA particles with free CHO groups on surface could be obtained<sup>[72]</sup>. These free aldehyde groups were transformed into primary amino, aromatic amino, and hydrazide groups by reaction with hexamethylene diamine, *m*-phenylene diamine, and adipic dihydrazide, respectively, in the presence of sodium cyanoborohydride. The amino and hydrazide functionalized PVAs were used in the immobilization of sugars such as maltose, *D*-( $\beta$ )-glucosamine, and heparin. The immobilized heparin maintained its anticoagulant property.

Recently, biologically active groups such as ammonium and phosphonium chlorides were covalently anchored on PVA through chloroacetyl group as shown in Eq. (15)<sup>[73]</sup>. Chloroacetylation of PVA (MW = 13–23 kDa, Hy = 98%) was conducted in a suspension in chloroform for 3 days at room temperature. The subsequent reactions, affording the ammonium and phosphonium chlorides, were carried out with triethylamine (TEA) and triphenylphosphine/tributylphosphine, respectively, in benzene at 80°C for 4 days. The biocidal assessment of these polymeric salts revealed their effectiveness toward *Escherichia coli*, *Pseudomonas aeruginosa*, *Shigella* sp., *Bacillus subtilis*, and *Bacillus cereus*; the polymeric triphenyl phosphonium salt exhibited the highest biocidal activity. For the latter polymeric salt, the inhibitory effect was in this order *E. coli* < *Trichophyton rubrum* < *B. subtilis* < *P. aeruginosa*. The remaining polymeric salts acted differently toward these bacteria. In general, their inhibiting potency increased with their concentrations.

Eq. (15)

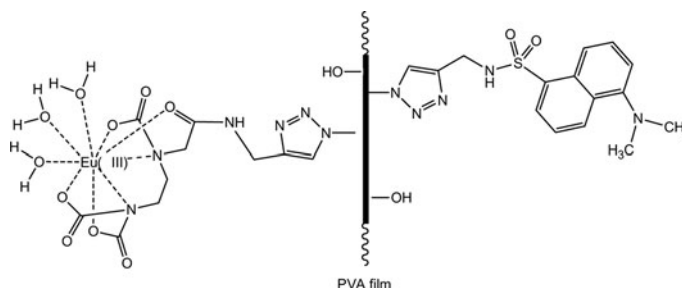
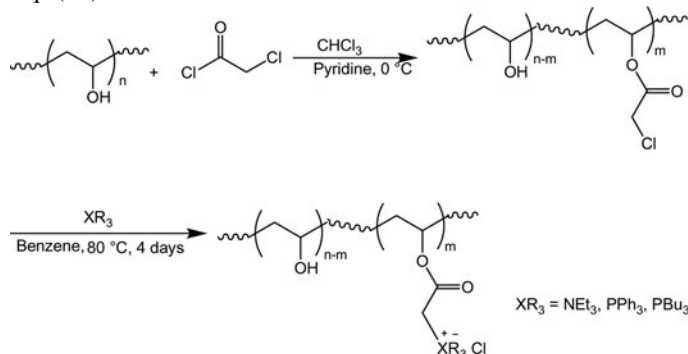


FIG. 5. CaDPA polymeric sensor based on functionalized PVA. Note: CaDPA, calcium dipicolinate; PVA, poly(vinyl alcohol).

In view of detecting *Bacillus anthracis*, a serious pathogen for the disease anthrax, and thus for human safety, Ma et al.<sup>[74]</sup> developed a polymeric sensor (Fig. 5) for calcium dipicolinate (CaDPA) which exists in the protective layers of bacterium. The detection was through fluorescence spectroscopy. PVA (DP = 2330, Hy = 87–89%) surface was subjected to tosylation and azidation, followed by binding a reference dye (from the reaction of dansyl chloride and propargylamine) and a probe ligand (EDTA-Eu(III)), via click chemistry protocol.

PVA grafted on multiwalled carbon nanotubes, PVA-g-MWCNT, and on graphene oxide, PVA-g-GO, were conceived as drug nanocarriers<sup>[75,76]</sup>. The drugs loaded by these nanomaterials were camptothecin (CPT) and ellagic acid, anticancer drugs. The water-insolubility handicap of these drugs was alleviated using such water-soluble nanocarriers, stemming from the hydrophilicity of grafted PVA. These drugs when loaded on these nanocarriers exhibited higher cytotoxicity than the free drugs. Besides, the cytotoxic activity of PVA-g-MWCNT/CPT exceeded that of PVA-g-GO/CPT.

The hydrophilicity and biocompatibility of PVA were exploited in making  $\text{C}_{60}$ -fullerene photosensitizers (Fig. 6) for photodynamic therapy<sup>[77]</sup>. To produce PVA-g- $\text{C}_{60}$  nanohybrids, poly(vinyl acetate) (PVAc) was developed as precursor via cobalt-mediated radical polymerization, and the PVAc-Co(acac)<sub>2</sub> reacted radically with  $\text{C}_{60}$  in 1,2,4-trichlorobenzene. Methanolysis of PVAc-g- $\text{C}_{60}$  led to PVA-g- $\text{C}_{60}$  (Fig. 7) with 2.6 wt% of  $\text{C}_{60}$  and a molecular weight of 27.9 kDa. This nanomaterial showed some photodynamic activity.

In the aim at fashioning biological membranes with a varying hydrophilicity/hydrophobicity ratio, Cavusoglu and

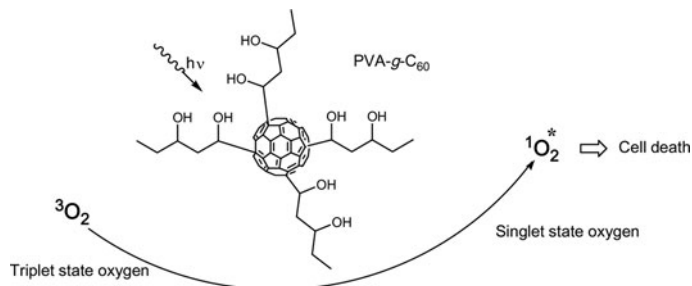


FIG. 6. PVA-g- $\text{C}_{60}$  photosensitizer for photodynamic therapy. Note: PVA, poly(vinyl alcohol).



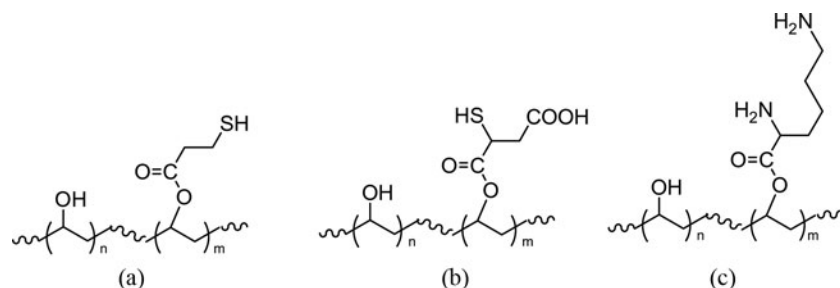
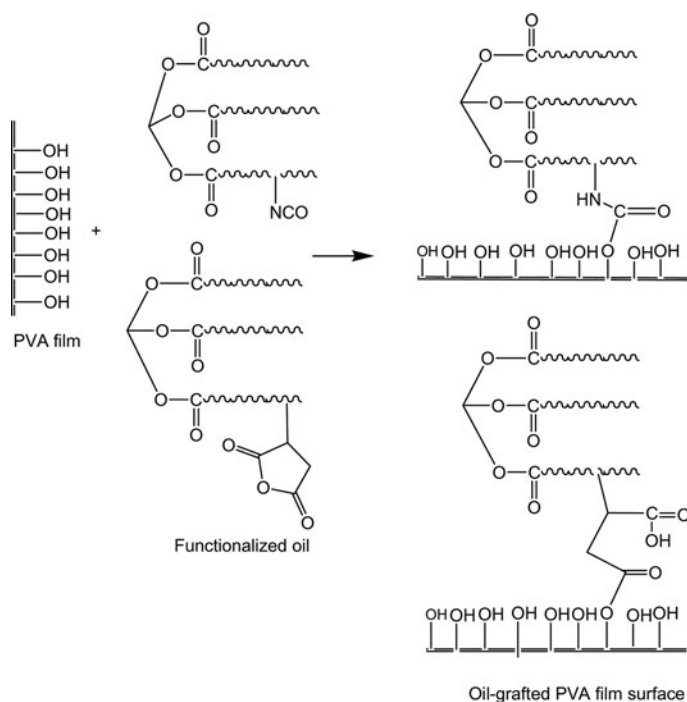


FIG. 7. (a) PVA-MPA, (b) PVA-MSA, and (c) PVA-Lys. Note: PVA, poly(vinyl alcohol); MPA, mercaptopropionic acid; MSA, mercaptosuccinic acid; Lys, lysine.

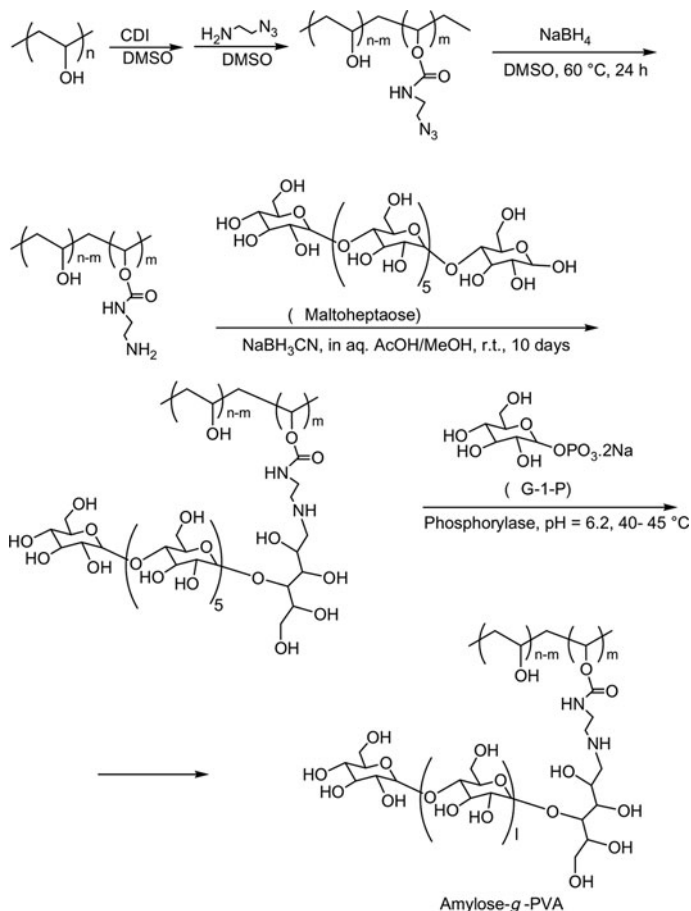
Kusefoğlu<sup>[78]</sup> modified PVA films (MW = 88 kDa, Hy = 98%) with soybean oil triglycerides functionalized with isocyanate and succinic anhydride groups (Eq. 16). PVA films were in contact with the functionalized oil in toluene and in the presence of DMAP as catalyst for 18–24 h at a temperature range of 60–90° C. The grafting occurred mainly on the film surfaces and through ester and urethane linkages. Water contact angle measurement, an indirect estimation of hydrophilicity/hydrophobicity extent of the ensued functionalized PVA films, was found to increase with concentration increasing of the functionalized oil, from about 50° for nongrafted film to about 90° for 6 and 33% by weight of the isocyanate and succinic anhydride groups, respectively; the lower concentration of the former hints at its higher reactivity with the secondary alcohol of PVA when compared with the latter one. In addition, this contact angle rose with the reaction temperature. A slight decrease in  $T_g$  was detected, from about 76°C for nongrafted PVA to about 73–74°C for the grafted ones, indicating low grafting degrees.

Eq. (16)



Amylose was successfully grafted onto PVA matrix via a multistep functionalization, including the activation of PVA (MW = 88.1 kDa) with CDI, followed by reaction with 2-azidoethylamine and the reduction with  $\text{NaBH}_4$ <sup>[79]</sup> (Eq. 17). The continuation of this protocol was to graft maltoheptaose to the thus-functionalized PVA in the presence of the reducing agent  $\text{NaBH}_3\text{CN}$ . The phosphorylase-catalyzed enzymatic polymerization of G-1-P ( $\alpha$ -D-glucose 1-phosphate disodium salt) in the presence of the resulting maltoheptaose-grafted PVA afforded amylose-grafted PVA. The molecular weight of the latter graft copolymer was about 129.9 kDa with a molecular weight of the grafted amylose of 34.8 kDa. Such amylose-g-PVA provided the formation of a transparent

Eq. (17)



film from an aqueous solution, a fact that was not achieved with amylose/PVA blend. The complex formed between molecular iodine and amylose-g-PVA was more stable than that between molecular iodine and PVA, and this was explained in terms of the embedding capacity of the amylose cavities of molecular iodine.

## ADSORPTION AND SEPARATION

Removal of toxic substances from potable water is undoubtedly mandatory. Polymers are viewed as essential materials in the separation of such hazardous contaminants, mainly, through sorption. The state-of-the-art uses of the polymeric materials are chiefly membranes and hydrogels. The contaminants are commonly heavy metals, cyanide, and dyes.

Functionalizing PVA stands as a valuable means for removal of nanosized metallic contaminants. Mahanta and Valiyaveetil<sup>[80]</sup> demonstrated the extraction efficiency of metals in their nanoforms by properly functionalized PVA nanofibers. For this purpose, they modified the surface of electrospun PVA nanofibers (300–500 nm) by esterification of the hydroxyl groups with mercaptopropionic acid (MPA), mercaptosuccinic acid (MSA), and lysine (Lys) in aqueous medium at 80°C. The thus-functionalized PVA nanofibers (Fig. 7) were cross-linked with glutaraldehyde to yield sorbing membranes with surface areas of  $5.30 \text{ m}^2 \text{ g}^{-1}$ . PVA–Lys membrane (C) showed an adsorption capacity toward silver nanoparticles greater than PVA–MPA (A) and PVA–MSA (B), about 90% for the former membrane against ~50% for the remaining membranes after 3 h. However, all membranes showed the same affinity toward gold nanoparticles, and the adsorption extents were nearly 90%. The adsorption capacity of the unmodified PVA nanofiber membrane was limited toward both metal nanoparticles, not exceeding 20%. Such difference behavior was explained by the hard–soft acid–base theory; sulfur being softer base and nitrogen a borderline one.

Magnetic nanoparticles  $\text{Fe}_3\text{O}_4$  (MNPs) were covalently attached to thiourea-functionalized PVA through epichlorohydrin functionality as pictured in Figure 8<sup>[81]</sup>. Functionalization of aminated MNPs (triethylenetetramine) was realized with epichlorohydrin, followed by reaction with PVA at alkaline pH, involving the opening of epoxy ring by hydroxyl group of PVA. A further treatment of PVA with epichlorohydrin allowed the reaction with thiourea. TGA analysis revealed a 47% of PVA attachment on MNPs. The obtained spherical MNP–PVA nanoparticles (13 nm) were superparamagnetic with a saturation magnetization of  $6.65 \text{ emu g}^{-1}$ . An adsorption capacity of the MNP–PVA toward  $\text{Pb(II)}$  ions was about  $50 \text{ mg g}^{-1}$  with a rate of  $12.45 \text{ mg g}^{-1} \text{ min}^{-1}$ , for a  $\text{Pb(II)}$  concentration of  $80 \text{ mg L}^{-1}$ , a contact time of 20 min, a temperature of 28°C, and a pH of 5.5. This adsorption fitted the Freundlich isotherm.

A mesoporous nanofiber membrane with a copper (II) adsorptivity was conceived by functionalizing the composite

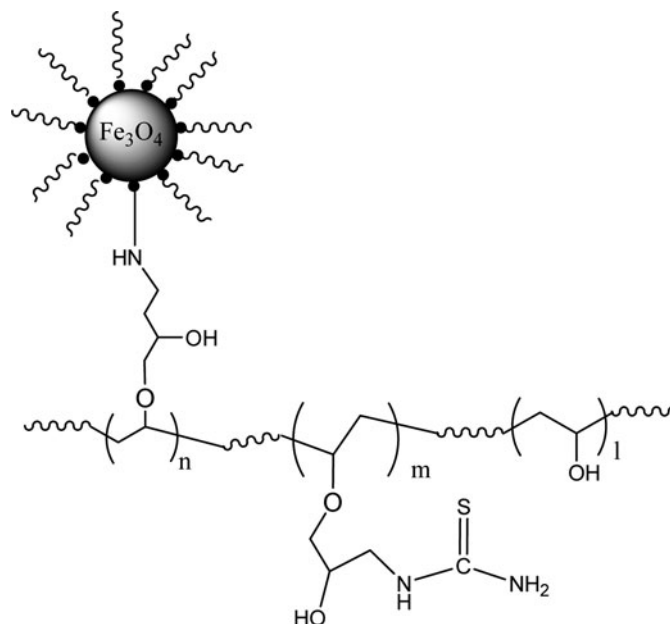


FIG. 8. Magnetic nanoparticle/thiourea-functionalized PVA hybrid, MNP–PVA nanoparticle. Note: PVA, poly(vinyl alcohol); MNP, Magnetic nanoparticle.

PVA/silica (Fig. 9b) using 3-mercaptopropyltrimethoxysilane (MPTMS)<sup>[82,83]</sup>. Toward this objective, a sol–gel technique was applied. The approach was to set a priori an aqueous gel formed by mixing MPTMS, tetraethyl orthosilicate (TEOS), cetyltrimethyl ammonium bromide (CTAB) as a template, absolute ethyl alcohol and poly(vinyl alcohol) (MW = 88–97 kDa, Hy = 99%) in acidic aqueous/ethanolic medium for about 4 h at 60°C. The thiol-functionalized PVA/ $\text{SiO}_2$  nanofiber membranes (diameter = 100–700 nm, pore volume  $\sim 0.3\text{--}0.5 \text{ cm}^3 \text{ g}^{-1}$ , pore diameter  $\sim 3\text{--}5 \text{ nm}$ , surface area  $\sim 295\text{--}474 \text{ m}^2 \text{ g}^{-1}$ ) and the PVA nanofiber membranes (diameter = 500–1,000 nm, pore volume  $\sim 0.65 \text{ cm}^3 \text{ g}^{-1}$ , pore diameter  $\sim 7 \text{ nm}$ , surface area  $\sim 522 \text{ m}^2 \text{ g}^{-1}$ ) were then completed by electrospinning technique. The removal of  $\text{Cu(II)}$  by the As-made composite membrane was pH-dependent, as the protonation of thiol groups may take place; the adsorption increased rapidly from a pH of 2–5, then slowly because of the inability of adsorption of the protonated thiol groups. An adsorption capacity of about  $490 \text{ mg g}^{-1}$  was measured at a pH of 5; that by pure PVA nanofiber membrane was nearly  $390 \text{ mg g}^{-1}$ . Iranian researchers<sup>[84–86]</sup> worked on making nanofiber membranes PVA/TEOS/ $\gamma$ -aminopropyl triethoxysilane (APTES) (Fig. 9a) and PVA/TEOS/MPTMS (Fig. 9b) under the sol–gel method for the removal of heavy metals, particularly  $\text{Cu(II)}$ ,  $\text{Cd(II)}$ , and  $\text{Ni(II)}$ , from water (The PVA to be functionalized was of a MW = 72 kDa and Hy = 99%). The effects of the functionalizing agent of PVA and the metallic ion on the metallic adsorption were proved to be evident. The physical properties of the As-prepared membranes PVA/TEOS/MPTMS and PVA/TEOS/APTES were, respectively, 152–182 and 153–282  $\text{m}^2 \text{ g}^{-1}$  in surface area, 0.26–0.36 and

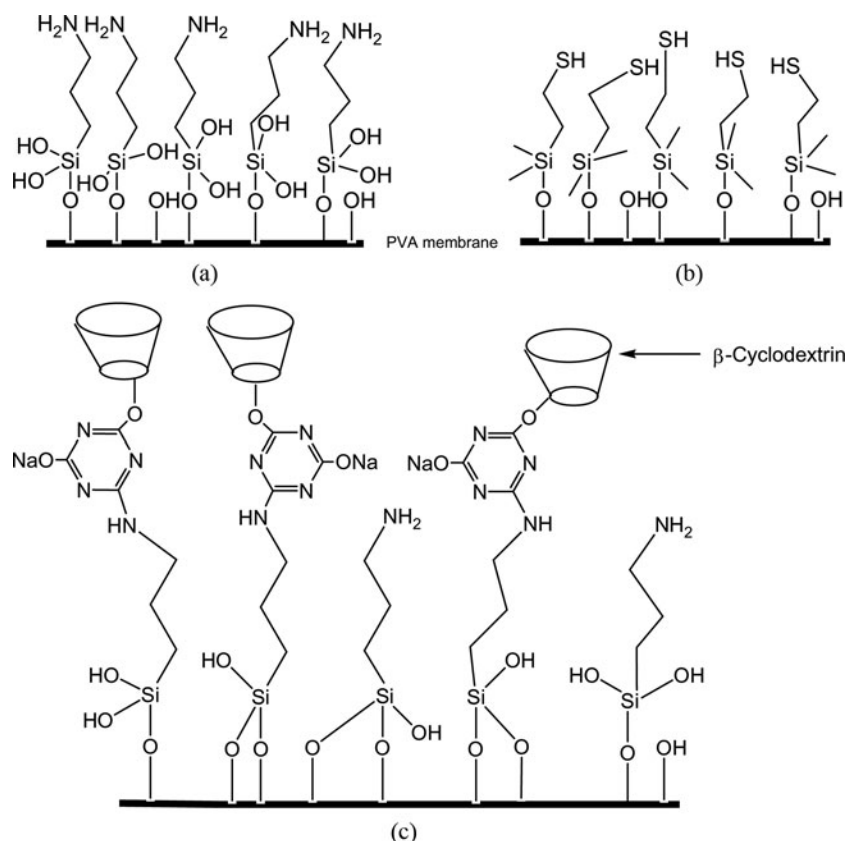


FIG. 9. (a) Aminosilylated PVA membrane surface, (b) thiol-functionalized mesoporous PVA/SiO<sub>2</sub> composite nanofiber membrane, and (c)  $\beta$ -cyclodextrin-functionalized mesoporous PVA/SiO<sub>2</sub> composite nanofiber membrane. Note: PVA, poly(vinyl alcohol).

0.25–0.52 cm<sup>3</sup> g<sup>−1</sup> in pore volume, and 2.00–2.60 and 4.62 nm in average pore diameter. In general, the adsorption capacity by PVA/TEOS/MPTMS was low for both Cd(II) and Ni(II), but that of Cd(II) was greater in all conditions. The removal extent did not exceed 61 and 10 mg g<sup>−1</sup> for Cd(II) and Ni(II), respectively, under optimal conditions: a MPTMS content of 15%, a TEOS content of 20%, an initial concentration of 100 mg L<sup>−1</sup>, a pH of 5, a temperature of 45°C, and a contact of 240 min. However, the adsorption capacity of the mesoporous PVA/TEOS/APTES nanofiber membrane toward Cd(II) was nearly 327 mg g<sup>−1</sup> under the following optimal conditions: a pH of 6, a contact of time of 90 min, and a temperature of 45°C. And, the Cd(II) adsorption isotherms fitted the Freundlich model in the case of PVA/TEOS/MPTMS, and the Redlich–Peterson one in the case of PVA/TEOS/APTES. The maximum adsorption capacity of PVA/TEOS/MPTMS toward Cu(II) was about 70 mg g<sup>−1</sup> under the optimal conditions cited for the case of Cd(II), that of PVA/TEOS/APTES with 10 wt% APTES was lower because its p*H*<sub>pzc</sub> (pzc = point of the zero charge) was higher (3.8) than that of the former membrane (3.1). As with Cd(II), Freundlich model was found to describe better the Cu(II) adsorption data.

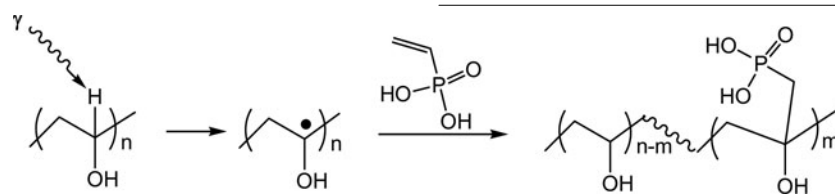
Nasir and Nur<sup>[87]</sup> functionalized PVA with MPTMS (Fig. 9) in view of embedding gold nanoparticles (20–180 nm). The

MPTMS-modified PVA was cast on a glass slide and the gold nanoparticles were spread on the dried functionalized PVA membrane by an annealing method. Analyses of the MPTMS-modified PVA/Gold films by field emission scanning electron microscopy (FESEM) and transmission electron microscopy (TEM) confirmed the presence of the gold nanoparticles complexed via thiol groups.

Exertion of irradiation on PVA may provoke the homolytic rupture of the CH of the –CHOH– group, leading to possible grafting of appropriate modifying molecules on the matrix at the carbon site without altering the secondary alcohol. Chi et al.<sup>[88]</sup> were able to make out an adsorbent for uranyl (IV) (UO<sub>2</sub><sup>2+</sup>) by grafting phosphonic acid groups on PVA fiber surfaces by means of irradiation. In this study, pristine PVA fibers were irradiated by  $\gamma$ -ray (88 Gy min<sup>−1</sup>) before addition of the solution of vinyl phosphonic acid in dioxane and the reaction was prolonged for 5 h at 80°C (Eq. 18). The optimal adsorption of UO<sub>2</sub><sup>2+</sup> by the As-functionalized PVA fibers was about 55% (32.1 mg g<sup>−1</sup>) at a pH of 4.5, a reaction of 30 min, and a temperature of 25°C. At pHs beyond 4.5, the adsorption capacity dropped because of the plausible presence of hydrolysis species (UO<sub>2</sub>OH<sup>+</sup>) and (UO<sub>2</sub>)<sub>2</sub>(OH)<sub>2</sub><sup>2+</sup>. It was advanced that the adsorption mechanism involved chelation of uranyl ions by both hydroxyl groups of PVA

and the phosphorous acid. The adsorption isotherm of uranyl by vinyl phosphonic acid-modified PVA fiber fitted the Langmuir model.

Eq. (18)



Guhanathan and his coworkers<sup>[89,90]</sup> modified PVA (MW = 14 kDa, Hy = 98–99%) with nitrogen heterocycles containing phosphorus, *N*-heterocyclic phosphonyl dichlorides. The latter compounds were achieved by reaction of nitrogen heterocycles (imidazole, indole, piperidine, piperazine, 1,2,4-triazole) with phosphorus oxychloride. Reaction of PVA with *N*-heterocyclic phosphonyl dichlorides, affording materials of Figure 10, was conducted in DMF at 90°C for 12 h, and in the presence of TEA. The degrees of functionalization were in the range of 51–74%. To one's surprise, the thus-modified PVAs, being cross-linked, were soluble in pyridine, DMF, and DMSO; virgin PVA is insoluble in pyridine and DMF.  $T_g$ 's were greater (96–204°C) than that of starting PVA (90°C), and  $T_m$ 's fluctuated between 132 and 233°C (that for PVA was measured as 185°C). The adsorption capacities of the different *N*-heterocycle-functionalized PVAs toward heavy metals were higher for Cd(II), Cu(II), Pb(II), Hg(II) among the studied ions. The adsorption capacity followed the heterocycle order: imidazole > piperidine > piperazine > indole > triazole. The adsorption capacity of the imidazole-modified PVA toward Cu(II) and Pb(II) was nearly 50–55 mg g<sup>-1</sup> at an optimal pH of 7. The limiting oxygen indexes (LOI) of the *N*-heterocyclic-phosphorus-modified PVAs were in the spectrum of 20–25, suggesting their higher flame retardancy when compared with that of the bare PVA (LOI = 17.5).

The grafting polymerization of diaminomaleonitrile in the presence of PVA at 50°C using ceric ammonium nitrate led to polydiaminomaleonitrile-graft-PVA<sup>[91]</sup>. The grafting yield

and grafting efficiency were optimal after 2 h of polymerization, 136 and 70%, respectively. The water uptake of the graft copolymer was 63%, compared to that of PVA (23%). Its mechanical properties were greater than those of PVA: tensile

strength of 42 MPa, elongation at break of 7.3%, against 24 MPa and 4.7%. The  $T_g$  of the graft copolymer was 58°C, a temperature lower than that of PVA (83°C), a fact stemming from the incorporation of methylene groups and the increase in free volume. The graft copolymer was more thermally stable than the pristine PVA; its degradation started at 330°C and that of PVA at 243°C. The graft copolymer was successfully exploited in the sorption of heavy metals via its amidoxime form (amidoximation of the cyano groups by reaction with hydroxylamine hydrochloride).

In view of facilitating the transfer of highly magnetic nanocrystals into an aqueous environment, Liong et al.<sup>[92]</sup> proved that PVA functionalized by carboxymethylation would impart a multidentate and strong chelation toward iron oxide. Carboxymethylation of PVA was realized with bromoacetic acid under alkaline condition; up to 510 μmol carboxymethyl groups per gram of carboxymethylated PVA could be introduced. The nanocrystals of MnFe<sub>2</sub>O<sub>4</sub> overlaid with oleate/oleylamine could be transferred using a dilute aqueous solution of tetramethylammonium hydroxide acting as phase transfer catalyst, displacing the oleylamine and oleic acid surfactants, and the presence of carboxymethylated PVA would infer a stable dispersion.

Recently, the removal of boron (mostly in the form of B(OH)<sub>3</sub>) from aqueous water could be accomplished through adsorption by PVA-functionalized activated carbon and CNTs<sup>[93]</sup>. The carbonaceous materials were both acidified with nitric acid before reaction with PVA in heterogeneous system at 60°C for 72 h; oxygenated functional groups were created, including hydroxyl, carboxyl, and lactone. Activated carbon and CNTs were functionalized with PVA of a molecular weight of 2 and 95 kDa, respectively. Surface areas measured for the functionalized carbonaceous materials were lower than those for the nonmodified materials: 216.7 and 172.1 m<sup>2</sup> g<sup>-1</sup>, respectively, against 576.5 and 193.0 m<sup>2</sup>/g. This surface area lowering was attributed to the micropores blocking of PVA chains. The boron adsorption capacity at equilibrium time (24 h) by activated carbon/PVA and CNT/PVA conjugates reached 0.94 and 1.22 mg g<sup>-1</sup>, respectively, values higher than those for the nonmodified materials, 0.73 and 0.37 mg g<sup>-1</sup>. Such adsorption improvement was explained in terms of

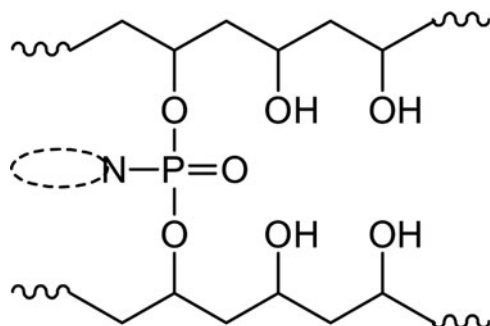


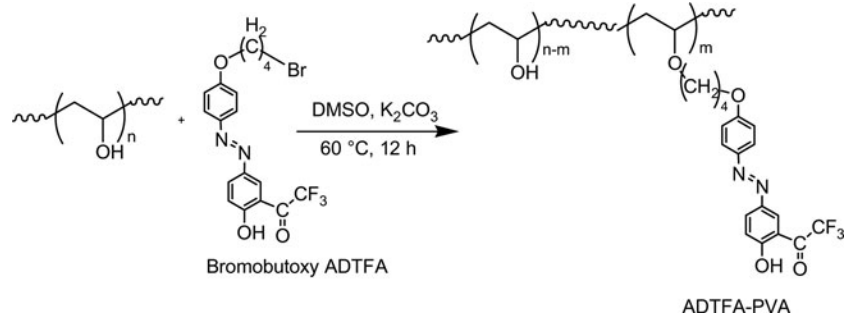
FIG. 10. PVA functionalized with nitrogen heterocycles containing phosphorus. Note: PVA, poly(vinyl alcohol).



favorable complexation of boron species by the hydroxyl groups of PVA. The effect of pH on the boron adsorption by these modified and nonmodified carbonaceous materials was not significant; yet, better adsorption extent was observed for slightly basic conditions.

For the purpose of cyanide detection in water, Isaad and Salaun<sup>[94]</sup> coupled 2,2,2-trifluoro-1-(2-hydroxyl-5-((4-hydroxyphenyl) diazenyl)phenyl) ethanone (ADTFA), as a chemosensitive dye and chemodosimeter, to PVA (MW = 16 kDa, Hy = 98–98.8%). The modification reaction involved the use of DMSO as a solvent and K<sub>2</sub>CO<sub>3</sub> as a base (Eq. 19). The reaction time of 12 h at 60° C afforded ADTFA–PVA in 53% yield. The ADTFA–PVA was effective in detecting cyanide ions in pure water as the trifluoroacetyl group can react selectively with cyanide ions in the presence of other ions such acetate and fluoride.

Eq. (19)



Surfaces of pervaporative membranes were designed from PVA (DP = 1750, Hy = 98%) functionalized with APTES for dehydration of ethanol<sup>[95]</sup>. It was either to cast APTES solution onto a prepared PVA membrane or by immersing the latter in the former solution at 30°C for a while. Mechanistically, acidic hydrolysis generated the reactive silanol groups which could condense with hydroxyl groups of PVA, affording ultimately a membrane of a balanced hydrophilicity (Fig. 9a). The intensity of X-ray diffraction (XRD) peak observed for pristine PVA at  $2\theta = 20^\circ$  decreased with increasing APTES and contact time; the slight peak shift denoted the reduction in crystallinity upon modification. The increase in the contact angle of the treated PVA membrane with increasing modifying agent content suggested that the membrane surface turned out to be less hydrophilic. The success of the modification was also proved by XPS analysis, revealing the chemical binding and functionality of treated PVA on the surface. The mechanical parameters of the treated membranes were enhanced, from a tensile strength of ~65 MPa and a Young's modulus of ~3795 MPa for the virgin PVA, to ~94 and ~5365 MPa, respectively. The best permselectivity performance in the pervaporative dehydration of ethanol was noticed for the PVA membrane modified with 1 wt% of APTES and a contact time of 120 min and a feed temperature of 60°C: a separation factor of about 80% and a permeation flux of about 0.40%.

Zhang et al.<sup>[96]</sup> valorized the As-Q-PVA [Q-PVA with a degree of quaternization (DQ) of 3.26%, see Eq. (22) below] and its cross-linked form (with glutaraldehyde), as hydrophilic membranes in the dehydration of ethanol by pervaporation technique. The quaternary ammonium functionality brought a reduction in crystallinity of PVA membranes. While the contact angle decreased of uncross-linked Q-PVA with increasing DQ, from ~70 (0% DQ) to from ~47° (4.04% DQ), that for the cross-linked increased with increasing degree of cross-linking (DC), from 51 (0% DC) to 56° (3.92% DC). With a rise in DQ for uncross-linked membrane the swelling of the membranes in 85% aqueous ethanol after 48 h at 50°C was found to rise of nearly 44%, and the rise in DC for the cross-linked one induced a drop of about 20–30%. The two pervaporative parameters, water permeability and permselectivity, of the uncross-linked Q-PVA membrane were found to increase

with increasing DQ. For 4.035% DQ, they were 12.628  $\text{g} \mu\text{m}^{-2} \text{h}^{-1} \text{kPa}^{-1}$  and 58.3, respectively. Those for the cross-linked membrane for a DC of 3.92% were 7.987  $\text{g} \mu\text{m}^{-2} \text{h}^{-1} \text{kPa}^{-1}$  and 75, respectively.

Esterification reaction between 4-sulfophthalic acid with PVA (MW = 125 kDa, Hy = 87.5%) led to a membrane (Fig. 11) for the pervaporative dehydration of isopropanol<sup>[97]</sup>. The functionalization extent varied from 5 to 20 wt%. The wide-angle XRD analysis was consistent with the fact that the functionalization/cross-linking with 4-sulfophthalic acid reduced the crystallinity of PVA, by breaking the hydrogen bonding between the hydroxyl groups. The glass transition

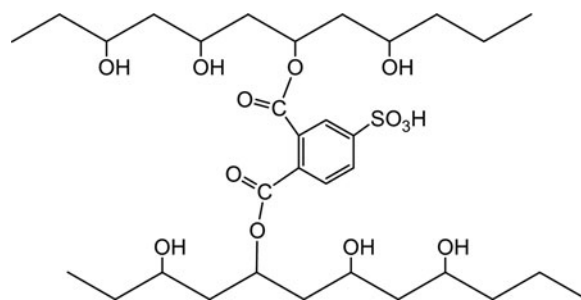


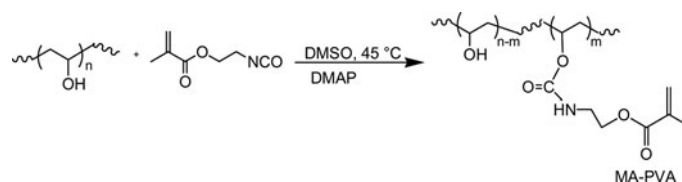
FIG. 11. Pervaporative membrane from esterified PVA with 4-sulfophthalic acid. Note: PVA, poly(vinyl alcohol).



temperature of the S-PVA ( $T_g > 85^\circ\text{C}$ ) was higher than that of innate one ( $T_g = 85^\circ\text{C}$ ), but the melting point  $T_m$  decreased from 228 to  $205^\circ\text{C}$ . And, while  $T_g$  increased with increasing functionalization degree as expected,  $T_m$  remained unchanged at  $205^\circ\text{C}$ . Functionalization/cross-linking with 4-sulfophthalic acid enhanced the thermal stability of the PVA membranes. The tensile strength of the As-made membranes increased from 65 MPa for untreated PVA to 239 MPa for 20% sulfonated one and their tensile elongation decreased from 383 to about 63%; these mechanical properties are in tune for use in pervaporation purpose. Swelling extents of the membranes with 5 and 20% 4-sulfophthalic acid in 70/30 isopropanol/water reached about 85%. The total flux for this pervaporation run at  $40^\circ\text{C}$  for this feed was nearly  $25 \times 10^{-2} - 28 \times 10^{-2} \text{ kg m}^{-2} \text{ h}^{-1}$ , and this was mainly due to the flux of water. The measured selectivity factors provide that the membrane with 15 wt% in 4-sulfophthalic acid afforded the best dehydration extent.

Shang and Peng<sup>[98]</sup> prepared a composite ultrafiltration (UF) membrane by adhering a thin layer of PVA (polymerization degree  $\text{DP} = 1799$ ) modified with toluene diisocyanate (TDI) through urethane functionality. To this end, polyether-sulfone support membrane was initially immersed into an aqueous solution containing PVA, sodium dodecyl sulfate, and sodium hydroxide, followed by immersion into cyclohexane solution of TDI. The performance of this UF membrane was examined for water flux and egg albumin retention, and the results were  $204 \text{ L m}^{-2} \text{ h}^{-1}$  and 100%, respectively, for a reaction time of 30 s. These parameters were affected by the concentrations of all reactants that is PVA, TDI, SDS, and NaOH. The antifouling capacity of this composite membrane was enhanced vis-à-vis the support membrane; the oil removal and water flux reached 92% and  $40 \text{ L m}^{-2} \text{ h}^{-1}$ , respectively, for the former membrane, against only 80% and  $20 \text{ L m}^{-2} \text{ h}^{-1}$  for the latter membrane. Moore et al.<sup>[99]</sup> patented a work on the hydrophilic membrane confection by covalently grafting monomers that are electron beam reactive groups, on PVA through either an ester or urethane linkage. These monomers are numerous and to cite but a few there are acryloyl chloride, maleic anhydride, 2-isocyanatoethyl methacrylate, itaconic anhydride, ethyl 2-cyanoacrylate, *N*-(hydroxymethyl)acrylamide, and GMA. The catalysts used included TEA, DMAP, and dibutyltin dilaurate (DBTL). The conversion of the different modifications fluctuated between 70 and 90% and the add-ons were in the range of 5–14 wt%. A typical example is illustrated in Eq. (20) where PVA is shown to react with 2-isocyanatoethyl methacrylate in DMSO or THF at  $45^\circ\text{C}$  and in the presence of DMAP to end up with methacrylate-modified PVA, referred to as MA-PVA. When subjected to electron beam (125 kV, 40 kGy), the aqueous solution of the MA-PVA deposited on PTFE membrane generated hydrophilic porous membrane; the add-ons were in the range of 5–14 wt%.

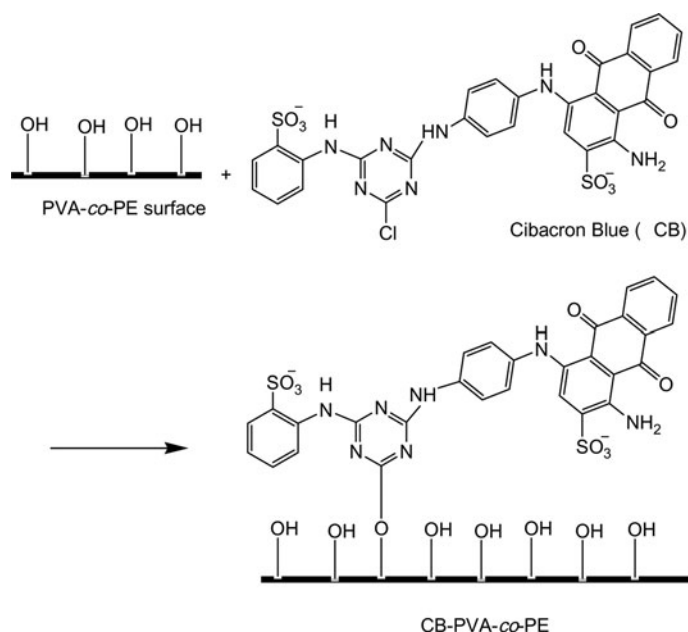
Eq. (20)



In 2012, the Chinese school<sup>[100]</sup> reported the potential adsorption capacity of PVA/TEOS/MPTMS nanofiber membranes toward indigo carmine and acid red dyes. The results of this study were that the adsorption profiles obeyed Langmuir, Freundlich, and Redlich–Peterson adsorption models. The adsorption capacity was  $\sim 267 \text{ mg g}^{-1}$  for indigo (for a concentration of  $500 \text{ mg L}^{-1}$ ) and  $\sim 212 \text{ mg g}^{-1}$  for acid red (for a concentration of  $315 \text{ mg L}^{-1}$ ) at a pH of 2 and a temperature of  $25^\circ\text{C}$ . The same sol-gel/electrospinning strategy for making  $\beta$ -cyclodextrin-functionalized mesoporous PVA/ $\text{SiO}_2$  nanofiber membranes (Fig. 9c) was adopted by Teng et al.<sup>[101]</sup> for the adsorptive removal of indigo carmine. The  $\beta$ -cyclodextrin could be grafted covalently to silylated PVOH by performing one-step co-condensation of TEOS and silylated monochlorotriazinyl- $\beta$ -cyclodextrin, in the presence of CTAB. The adsorption capacity of nanofiber membrane (Fig. 10c) ( $450\text{--}495 \text{ mg g}^{-1}$ ) toward the dye was about five times that of Figure 9a ( $90\text{--}100 \text{ mg g}^{-1}$ ) for a concentration of the adsorbate of  $100 \text{ mg L}^{-1}$  and at a pH of 5.2 and at room temperature.

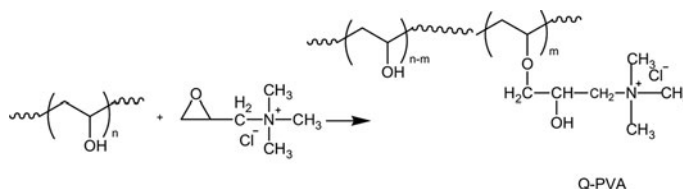
In view of designing a bio-detector in separation and purification techniques, Zhu et al.<sup>[102]</sup> immobilized Cibacron Blue F3GA on the surface of poly(vinyl alcohol-co-ethylene) (PVA-co-PE) nanofibrous membranes (50–300 nm) through hydroxyl groups of the PVA blocks. The solution of PVA-co-PE nanofibers and the dye were treated with NaCl for 1 h at  $60^\circ\text{C}$ , followed by treatment with NaOH for 4 h at  $80^\circ\text{C}$  as shown in Eq. (21). The presence of NaCl promoted the physical adsorption onto the PVA-co-PE nanofibers surfaces, hence allowed the covalent immobilization of the dye; NaCl, an electrolyte that reduced the electrical repulsion between the negatively charged dye molecules and nanofibrous membranes. At a concentration of  $1 \text{ mg L}^{-1}$  of Cibacron Blue F3GA, the maximum amount of covalently attached dye molecules was about  $\sim 225 \text{ mg g}^{-1}$  of nanofiber after optimal conditions: contact time of 4 h and pH of 11–12. The adsorption of BSA, a biological material, on the CB-PVA-co-PE nanofibrous membrane was successful, whereas it did not occur on the PVA-co-PE one. The greatest extent of adsorbed CB was about  $105 \text{ mg g}^{-1}$  after 1.5 h under the following conditions: pH of 5.0, temperature of  $25^\circ\text{C}$  and the initial BSA concentration of  $2 \text{ mg mL}^{-1}$ . At pHs lower and higher than 5, the adsorption capacity was low. An ionic strength of as low as 0.25 M of NaCl reduced the adsorption efficiency to about  $38 \text{ mg g}^{-1}$ , a decrease of 65%.

Eq. (21)



Fatehi et al.<sup>[103,104]</sup> studied thoroughly the functionalization PVAs with glycidyltrimethylammonium chloride to obtain quaternized PVAs, and studied the adsorption of these polymeric ammonium salts on cellulose fiber. These salts were the result of the reactions of PVA (MW = 9–10 kDa, Hy = 80%; MW = 124–186 kDa, Hy = 99%) with glycidyltrimethylammonium chloride in water at 80°C for a time of 60–210 min as given in Eq. (22). The degree of modification and the charge density (the number of quaternary ammonium groups) of the functionalized PVA (Q-PVA) were  $\sim 0.50$ – $5.00\%$  and  $\sim 0.10$ – $0.70$  mEq g<sup>-1</sup>, respectively. The adsorption extent of Q-PVA on cellulose was dependent on the molecular weight of the starting PVA and the charge density, and varied with the polymeric salt concentration; the lower the molecular weight of PVA and the charge density of the polymeric salt, the higher the adsorption extent. The adsorption capacity peaked at  $\sim 85$  mg g<sup>-1</sup> and  $\sim 300$  mg g<sup>-1</sup> for PVA of high and low molecular weights, and 600 and 2 000 mg L<sup>-1</sup> for the corresponding Q-PVAs, and for a charge density of as low as 0.18 mEq g<sup>-1</sup>. That for Q-PVA of higher charge densities was lower and decreased with increasing concentrations after reaching  $\sim 60$ – $80$  mg g<sup>-1</sup>. The ionic strength of polymeric salt solutions lowered the adsorption efficiency. All the results were explained in terms of affinity and repulsion between oppositely charged sorbate-sorbent. The adsorption characteristic of the PVA ammonium salts was exploited in the enhancement of mechanical properties of rice straw fibers and paper, as dry strength additives<sup>[105,106]</sup>.

Eq. (22)



Kara et al.<sup>[107]</sup> investigated the diffusion of the pyrene-PVA through agarose gel by virtue of its fluorescent property and water solubility. In both sorption and desorption, two kinds of diffusion occurred, coined short time diffusion ( $D_s$ ) and long time diffusion ( $D_l$ ) which were characterized by two diffusion coefficients. For 50 mg of agarose gel,  $D_s$  and  $D_l$  were measured as  $3.19 \times 10^{-6}$  and  $1.52 \times 10^{-6}$  cm<sup>2</sup> s<sup>-1</sup>, respectively, for the sorption process, and  $4.61 \times 10^{-6}$  and  $2.49 \times 10^{-6}$  cm<sup>2</sup> s<sup>-1</sup> for the desorption one.

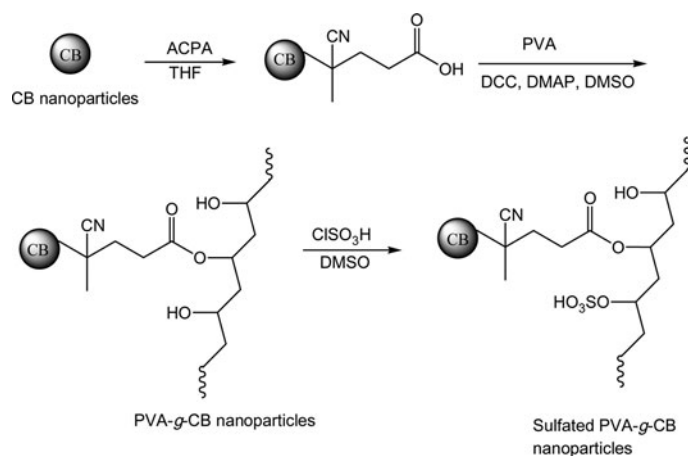
Sridhar and Oh<sup>[108]</sup> developed a method to separate the partially reduced graphene oxide from pure graphene by coagulation technique using an indirectly functionalized PVA. The addition of PVA to a mixture of these two graphenes allowed the separation, PVA reacting with partially reduced graphene oxide to form a gelatinous sticky precipitate. Mechanistically, PVA was thought to form strong hydrogen bonding with the GO, ending to the formation of a graphene-reinforced PVA hydrogel, GO acting as cross-linker.

Sun and his coworkers<sup>[109,110]</sup> applied the PVA functionalization to the capillary columns for electrophoresis of proteins. The silica capillary was aminated with (3-aminopropyl)trimethoxysilane, followed by reaction with glutaraldehyde, and finally the free aldehyde groups were acetalized with PVA. With these PVA-immobilized capillary columns, separations of cationic and anionic proteins were successful.

Tour and his coworkers<sup>[111]</sup> extended their research work on the application of nanoparticles in the oil-field industry to carbon black nanoparticles (CB NPs) functionalized with PVA. In the aim to determine the content extent of oil in the downhole well, novel approach is to transport “hydrocarbon compounds” acting as “probe molecules” through nanomaterials called “nanocarriers”. One of the promising candidates in this issue is the use of CB nanoparticles on which PVA chains (MW = 50 kDa) are appended. To achieve such goal, CB NPs were first treated with 4,4'-azobis(4-cyanopentanoic acid) (ACPA) to provide carboxyl groups, followed by esterification with PVA applying DCC strategy, affording PVA-g-CB NPs (200–300 nm) (Eq. 23). And, in view to ensure the stability of surfactants in the conditions of high temperature and salinity of the well, sulfatation of the grafted PVA chains was performed with ClSO<sub>3</sub>H. On the opposite to the highly sulfated PVA-g-CB NPs, the lightly ones were more efficient as far as stability was concerned in media of high salinity such as standard brine (pH = 6.4) even at elevated temperature, up to 100°C. In addition, the highly sulfated PVA-g-CB

NPs tended to aggregate because of their high zeta potential  $\zeta = -51.5$  mV, forming intermolecular links with rock surface, hence preventing the transport of the probe molecules. The lightly ones which had  $\zeta$  of  $-9.6$  mV had more mobility, thus a good transport efficacy. Experimental trials on the hydrocarbon detection by these NPs using triphenylamine as molecular probe revealed their good performance.

Eq. (23)



## CATALYSIS IN CHEMICAL REACTIONS

Catalyst-supported polymers have been designed and used since the dawn of use of polymeric reagents in organic synthesis<sup>[8,9,112]</sup>. In 2009, a Spanish school reported the use of PVA bearing sulfonic acid function (Fig. 13) as catalyst in the methoxylation of  $\alpha$ -pinene<sup>[113]</sup>, the esterification of fatty acids<sup>[114]</sup>, and the hydrolysis of sucrose<sup>[115]</sup>. The esterification of PVA (MW = 72 kDa) with sulfosuccinic acid leading to polymeric catalyst (Fig. 12), proceeded at two temperatures: at room temperature for 24 h, followed by a temperature of 120°C for a second 24 h. The methoxylation of  $\alpha$ -pinene with methanol in the presence of the sulfosuccinated PVA at 60°C led to  $\alpha$ -terpinylmethyl ether as a major product and several by-products. The reaction conversion increased with increasing functionalization up to 20 wt% sulfosuccinic acid. In view of realizing biodiesel from animal fats, a preliminary

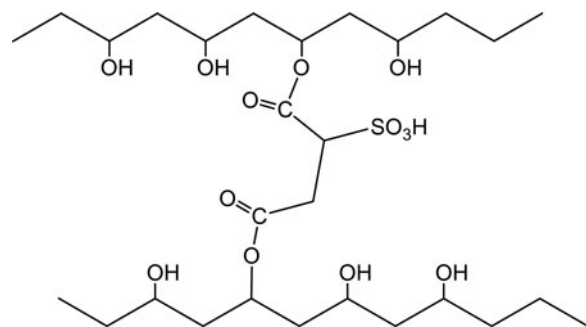


FIG. 12. Sulfosuccinated PVA. Note: PVA, poly(vinyl alcohol).

work was the feasibility of the esterification reaction of palmitic acid with methanol at 60°C using PVA functionalized with 40 wt% of sulfosuccinic acid as catalyst. The conversion of such reaction peaked 94% after a reaction time of 2 h. The better catalytic activity of the S-PVA when compared to that of sulfonated poly(styrene-*co*-divinylbenzene) toward the same esterification reaction was assigned to the hydrophilic–hydrophobic balance of the former. The catalysis of the hydrolysis of sucrose with PVA functionalized with 40 wt% of sulfosuccinic acid proceeded with high conversion (90%) to glucose and fructose after 3 h at 80°C. The sucrose conversion increased with increasing temperature, catalyst loading, and with prolonging time. In all cases of use, the catalytic activity of PVA functionalized with sulfosuccinic acid was almost retained after several runs.

A good catalytic activity of Fe(III)-5,10,15,20-tetrakis(pentafluorophenyl)porphine (FeTFPP) immobilized on pyridyl-functionalized PVA (Fig. 13) in the oxidation reaction of substrates such as veratryl alcohol, a lignin model compound, by hydrogen peroxide, was reported<sup>[116]</sup>. Toward this goal, acetalization of PVA (MW = 30–50 kDa, Hy = 100%) was accomplished with 4-aminobutylaldehyde diethyl acetal in acidic medium, followed by the reaction with 4-pyridine-carboxaldehyde to afford pyridyl-functionalized PVA with

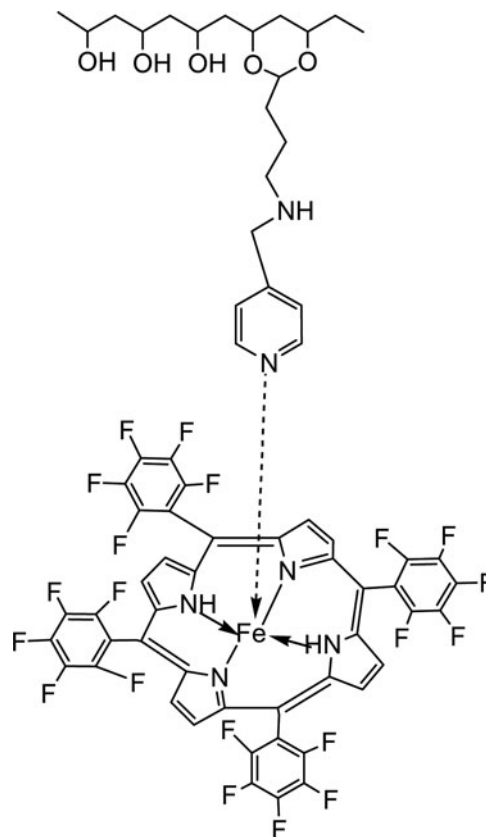
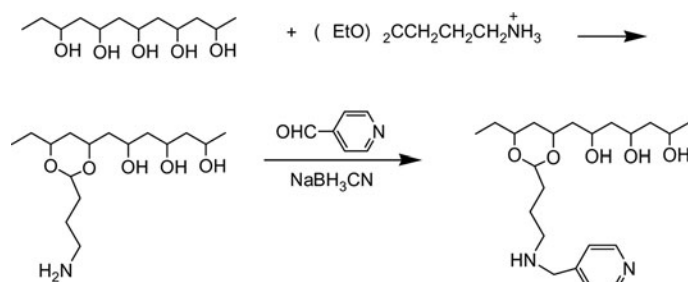


FIG. 13. FeTFPP-supported on pyridyl-functionalized PVA. Note: FeTFPP, Fe(III)-5,10,15,20-tetrakis(pentafluorophenyl)porphine; PVA, poly(vinyl alcohol).

high functionalization degree ( $>70\%$ ) (Eq. 24). The conversion of the oxidation of veratryl alcohol in the presence of the FeTFPP/pyridyl-functionalized PVA was  $\sim 68\%$  at  $\text{pH} = 3$ , and lower than 20 at  $\text{pH} \geq 4$ . However, the conversions for the case of azure B were higher even at higher pHs, 50–90%. Zucca et al.<sup>[117]</sup> extended the use of this bioinspired immobilized ferriporphine to the oxidation of hydrogen sulfide ion ( $\text{HS}^-$ ) by hydrogen peroxide; the conversion to sulfate ions attained 70% in 24 h when working at acidic pHs at room temperature, and the catalytic activity of the porphine neared 100% at a pH of 5. Thus, the application of such a technique to the  $\text{H}_2\text{S}$  removal in a large scale has been claimed as a feasible alternative.

Eq. (24)



A mutual  $\gamma$ -irradiation ( $0.5 \text{ kGy h}^{-1}$ ) of a dry PVA membrane/methanesulfonic acid system, at room temperature, afforded functionalized PVA membrane with a good catalytic capacity<sup>[118]</sup>. The temperature programmed pyrolysis-mass spectrometry analysis suggested the existence of free sulfonic acid (Fig. 14a) and the intramolecular and intermolecular sulfonates (Fig. 14b and 14c). The water contact angle decreased with increasing functionalization for a radiation dose ranging from 4 to 10 kGy. At higher doses (40 kGy), the very low water contact angle was due in part to the PVA scission. This catalytic ability of the sulfonic acid-functionalized PVA membrane was demonstrated in the esterification of isoamyl alcohol with acetic acid. The catalytic activity was linked with the used irradiation dose; it decreased with increasing dose and this was attributed to higher grafting (higher sulfonic acid content) at lower doses. A substantial decline in catalytic activity was noted after four runs.

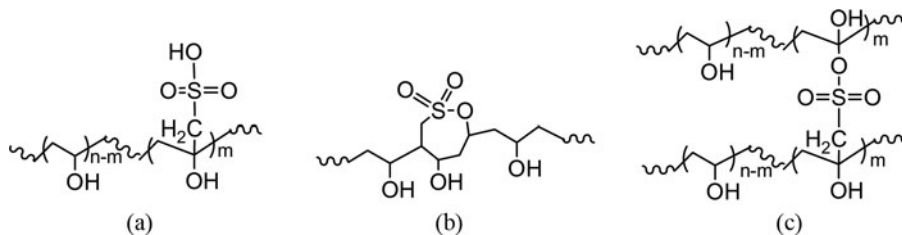


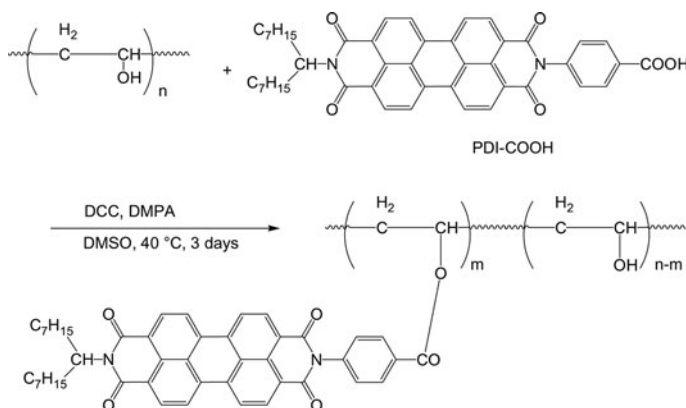
FIG. 14. The different products of  $\gamma$ -irradiation of PVA/methanesulfonic acid mixture. Note: PVA, poly(vinyl alcohol).

## MISCELLANEOUS FUNCTIONALIZATIONS AND APPLICATIONS

### Functionalization Through Ester Linkage

Modification of PVA is usually conceived through esterification of the hydroxyl groups because the reaction is straightforward. Salavagione et al.<sup>[119]</sup> were able to affix a perylenediimide derivative onto PVA backbone via an esterification reaction as pictured in Eq. (25). The reaction involved a mixture of PVA (MW = 89–98 kDa, Hy = 99%), *N*-(carboxyphenyl)-*N'*-(8-pentadecyl)peryene-3,4:9,10-bis(dicarboximide) (PDI-COOH), DCC and DMAP in DMSO. The perylenediimide-functionalized PVA with a modification degree of 22% was soluble in DMSO and hot water. The impact of such functionalization was an increase in  $T_g$  (from 82 to about  $91^\circ\text{C}$ ), a decrease in  $T_m$  (from 225 to  $179^\circ\text{C}$ ), and a reduction in the degree of crystallinity (from 51 to 24.5%). The perylenediimide-functionalized PVA was found to show photoluminescence property in DMSO solution ( $\lambda = 470 \text{ nm}$ ) as well as in solid state, a property of the functionalizing agent.

Eq. (25)



Mukherjee<sup>[120]</sup> reported the carboxymethylation of PVA in view of assessing the calorimetric aspect of the membrane made therefrom. Reaction of PVA with monochloroacetic acid in water in the presence of KOH at  $65^\circ\text{C}$  led to carboxymethylated PVA, with about 91% conversion. Such carboxymethylation extent engendered a substantial improvement in mechanical properties of PVA, that is, a tensile strength



of about 174 MPa for carboxymethylated PVA against about 59 MPa for untreated one. Also, the melting point of the former was higher than that of the latter, 207 against 202°C. Both of these observations were explained in terms of intensive intermolecular hydrogen bonding created by the carboxymethyl groups.

Ionic liquids were evaluated as alternative media for the esterification and urethanation of PVA in the aim at enhancing the functionalization outcome<sup>[121]</sup>. The esterifications of PVA (MW = 89–98 kDa, Hy > 99%) with acid chlorides such as acetyl chloride, octanoyl chloride, heptafluorobutyryl chloride, pentadecafluorooctanoyl chloride were run in 1-butyl-3-methylimidazolium chloride (BMIM-Cl) or tri-*n*-butylethylphosphonium diethylphosphate (TBEP-DEP) at 90°C in the presence of pyridine acting as catalyst and acid absorber. The reactions were rapid to reach high levels of modification (>95%), even in the absence of catalyst, and particularly in BMIM-Cl; while the reaction time in the case of TBEP-DEP was 1 h, that in the case of BMIM-Cl was only 10–15 min. *N,N*-dimethylpropylene urea, a cyclic urea, was used as solvent for the esterification of PVA (MW = 108 kDa, Hy = 99.7%) and poly(vinyl acetate-*co*-vinyl alcohol) with 3,5-dinitrobenzoyl chloride<sup>[122]</sup>. The copolymer was synthesized by transesterification using sodium methoxide. The esterification was carried out at 55°C for a time range of 5–160 h. The degree of esterification was high, 80–86%. The results showed that 80% of substitution degree could be achieved in only 5 h and the use of pyridine did not improve it. The glass transition temperatures of the esterified polymers were found to increase with increasing degree of substitution, up to 120–145°C, hinting at a stiffness gaining by the modification with bulkier dinitrobenzoyl groups.

PVA (MW = 33 kDa, Hy = 90%) reacted with benzoyl chloride in the presence of TEA under reflux for 3 h to afford benzoylated PVA (MW = 81 kDa) with 50% conversion<sup>[123]</sup>. The benzoylated PVA/carbon black composite was proved to possess a chemical vapor sensing property greater than untreated PVA/carbon black one. Yet, such property is chemical dependent; both composites have low sensitivity toward hexane and toluene vapors (low polarity), and the first composite showed higher sensitivity toward *iso*-propanol, THF, ethylacetate, dioxane, methanol, ethanol, acetonitrile, and DMSO vapors (high polarity). However, the latter composite did exhibit appreciable sensitivity toward methanol and water vapors. The sensitivity of benzoylated PVA/carbon black composite toward water vapors was insignificant.

Wang et al.<sup>[124,125]</sup> addressed the ability of the trimellitate PVA to possess anti-Hofmeister series property (Hofmeister or lyotropic series are a series of salts having an effect on the solubility of proteins, that is their salting-out property). The trimellitate PVA was formed by reaction of PVA (MW = 86 kDa, Hy = 99–100%) with trimellitic anhydride in DMSO and in the presence of TEA and DMAP at room temperature for 24 h. It was claimed that the esterification with the free

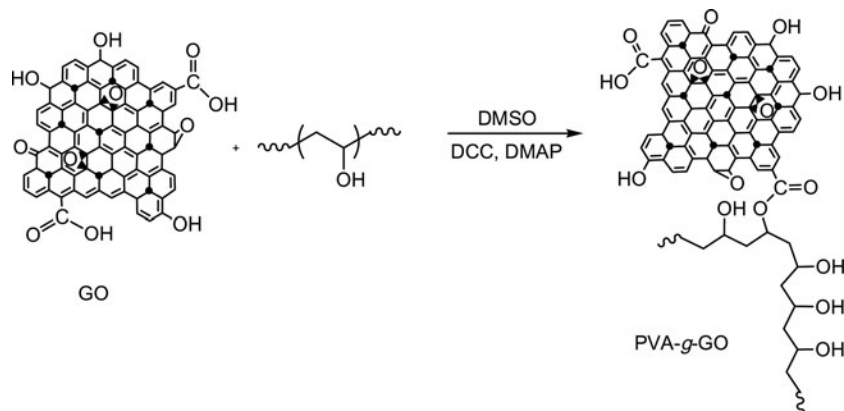
carboxylic acid group of the trimellitic anhydride was not significant under the mild conditions used. The degree of esterification reached 73%. The esterification of PVA with phthalic anhydride under the same reaction conditions gave rise to a 75% of esterification degree. Hydrogels made by inducing cross-linking of the trimellitate PVA solution in DMF with ethylene glycol diglycidyl ether at 70°C for 24 h showed a salting-in effect (anti-Hofmeister property). This was demonstrated by immersing the gel into Na<sub>2</sub>SO<sub>4</sub> solution; a water content in the gel attained 98%. General findings were the salting-in effect was observed in this order of anions and cations: SO<sub>4</sub><sup>2-</sup> > SCN<sup>-</sup> > Cl<sup>-</sup> and Li<sup>+</sup> > Na<sup>+</sup> > K<sup>+</sup>, an anti-Hofmeister order.

Functionalization of graphene forms with polymers was well-documented by Salavagione and his group<sup>[126]</sup>. Graphene sheets could not be functionalized but could be dispersed with polymer matrix to produce materials with better properties such as mechanical ones<sup>[127]</sup>; indeed, the presence of 1.8 vol.% of graphene within PVA (MW = 100 kDa) engendered a nanocomposite with 150% increase in tensile strength, 73% increase in Young's modulus, and a 220% decrease in strain at break. However, oxidation of graphene, commonly with nitric acid, renders it chemically reactive, known as graphene oxide. GO contains oxygenated functions including hydroxyl, epoxy, ketone, and carboxyl groups. The latter groups were exploited in the functionalization of GO with PVA by esterification. This esterification is usually activated using DCC. Nanocomposites were fashioned by incorporating PVA-functionalized graphene oxide (PVA-*g*-GO) in proportions as low as 0.5–2 wt% to pure PVA<sup>[128]</sup>. The PVA-*g*-GO were prepared by reacting GO nanosheets (1.5–2.0 nm in thickness) with PVA (MW = 61 kDa, Hy = 98.8–98%) in DMSO using DCC and DMAP as catalysts, at 50°C for 3 days (Eq. 25). The grafting efficiency was about 30%. The *T<sub>g</sub>*, *T<sub>m</sub>*, and *T<sub>c</sub>* of the PVA-grafted GO/PVA nanocomposites were greater than those of PVA, 74.5–80.3°C, 220.4–223°C, and 198.4–203.5°C, respectively, against 72.2°C, 211.8°C, and 196°C. The *T<sub>g</sub>* increase was reasoned as to be due to the reduced mobility of PVA chains by the PVA-*g*-GO rigid nanofiller. Better thermal stability of the nanocomposites *vis-à-vis* pristine PVA and GO was observed. The mechanical properties (tensile strength, Young's modulus, elongation at break) of the As-prepared nanocomposites were superior to those of virgin PVA: ~32–46 MPa, ~0.25–0.53 GPa, ~147–167%, respectively, against ~23 MPa, ~0.16 GPa, ~130%; the account for such observation is the strong interfacial affinity between PVA-*g*-GO and PVA matrix, resulting from the existing hydrogen-bonding and their better miscibility. Veca et al.<sup>[129]</sup> applied the same carbodiimide-activated esterification to the functionalization of carbon nanosheets (5 nm in thickness) with 2 mol% of carboxylic groups with PVA (MW = 70–90 kDa) as in Eq. (26). The PVA-grafted carbon nanosheet was easily dispersed in DMSO and hot water. Its *T<sub>g</sub>* was 90°C, higher than that of PVA (70°C), which



was explained in terms of mobility reduction of the PVA chains upon appending to graphene layers.

Eq. (26)



Hu and his coworkers<sup>[130]</sup> studied the dielectric properties of nanocomposites consisting of GO in its reduced form. The synthesized PVA-g-GO (25 wt% PVA) was subjected to the reduction with hydrazine affording (PVA-g-GO<sub>red</sub>). The latter hybrid material was more thermally stable than PVA and PVA-g-GO. The nanocomposites consisting of poly(vinylidene fluoride)/PVA-g-GO<sub>red</sub> were of high dielectric constant (230) and low loss factor (0.5) at the imposed frequency.

Grafting of PVA on graphene was reported to be induced by ultrasonic irradiation<sup>[131]</sup>. The heterogeneous mixture of PVA (MW = 146–186 kDa, Hy = 99%) and graphene (~1.2 nm in thickness) in water was subjected to ultrasonic irradiation (300 W) for 2 h, where PVA chains were broken homolytically. The PVA macroradicals would attack the graphene layers at the sp<sup>2</sup> hybridized carbons and via the “grafting to” strategy, giving rise to PVA-g-graphene. This nanomaterial (~3.8 nm in thickness) contained about 35 wt% PVA. It was readily dispersed in water, a dispersion that has been stable for two months at room temperature, and resulted in an insoluble black precipitate upon pouring into an excess of THF. The films cast from a mixture of PVA-g-graphene were homogeneous and with enhanced mechanical properties: a tensile strength of 98 MPa and a Young’s modulus of 5.2 GPa, and those of PVA were 56 MPa and 3.4 GPa, respectively. However, their strain at break and crystallinity extent were lower: 38 and 22% against 50 and 32%, respectively.

Salavagione et al.<sup>[132]</sup> esterified GO with PVA through carboxylic and acyl chloride functionalities, GO-COOH and GO-COCl. The PVA-g-GO materials, obtained with low degrees of grafting (1.8%), were soluble in hot water and hot DMSO. The conspicuous bands of GO in the Raman spectrum of PVA-g-GO’s appeared at 1320 and 1596 cm<sup>-1</sup>. Also, analysis revealed that the esterification took place at the isotactic configuration of PVA. The crystallinity degree of the latter decreased upon grafting to 0.51% without melting point. 35 and 12°C increases in the glass transition temperature

were observed for PVA-g-GO from GO-COOH and PVAOCl, respectively; graphene layers would have impeded the mobility of PVA chains.

Surfaces of carboxylated multiwalled carbon nanotubes (MWCNT-COOH) obtained by nitric acid treatment were modified by esterification with PVA at 140°C for 3 days<sup>[133]</sup>, producing a MWCNT-PVA hybrid as a black solid. Some changes in morphology for MWCNT-PVA were noticed upon standing for seven days in Tris-HCl buffer solution (2-amino-2-hydroxymethyl-propane-1,3-diol); no changes in microstructure and morphology occurred for MWCNT and MWCNT-COOH. Moreover, the dissolution of PVA-g-MWCNT started at the 21st day of dispersion and the analysis by HR-TEM (High-resolution transmission electron microscopy) showed that the CNT layers were decomposed to amorphous carbonaceous debris. Fu and Gu<sup>[134]</sup> fabricated composite fibers from PVA-g-MWCNT and PVA by gel spinning and hot-drawing processes. The drawn PVA-g-MWCNT/PVA fibers, obtained with a degree of crystallinity of 69.2%, exhibited better mechanical properties than pure PVA ones: tensile strength of 2.1 GPa, Young’s modulus of 34.1 GPa, and elongation of 10.3% against 1.2 GPa, 25.2 GPa, and 10.5%.

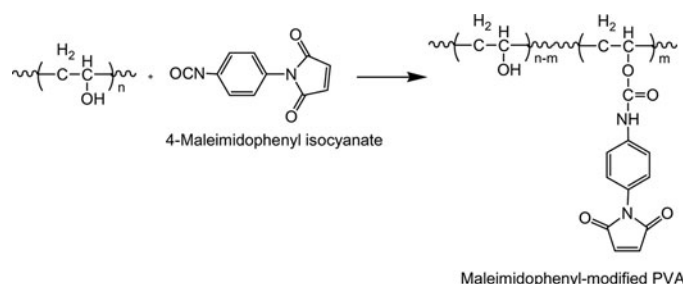
GO nanosheets and PVA films could be assembled layer-by-layer (LBL) through hydrogen-bonding interaction to form novel materials with the brick-and-mortar arrangement<sup>[135]</sup>. The LBL structure of these (PVA/GO)<sub>n</sub> nanocomposites was successfully confirmed by several analytical techniques, including XRD, XPS, FESEM, and atomic force microscopy (AFM). The thickness of a bilayer was found to be about 3 nm. The mechanical properties of (PVA/GO)<sub>300</sub>, elastic modulus and hardness, were improved *vis-à-vis* those of pure PVA: 17.64 GPa and 1.15 GPa, respectively, against 8.88 GPa and 0.34 GPa; that is, 98.7 and 240.4% increases in elastic modulus and hardness, respectively.

### Functionalization Through Urethane (or Carbamate) Linkage

Via urethane linkage, maleimidophenyl entity was covalently incorporated into PVA matrix as illustrated in Eq. (27)<sup>[136]</sup>. The realization of such modification was to carry out the

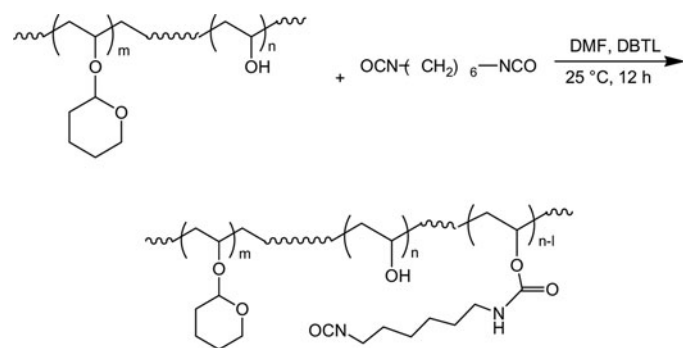
reaction of PVA (molecular weight MW = 67–85 kDa, Hy = 98%) with 4-maleimidophenyl isocyanate in DMF at 60°C and in the presence of DBTL as catalyst. The optimal substitution degree was about 35%. The maleimidophenyl groups affected the thermal behavior of the pristine PVA; the glass transition temperature  $T_g$  dropped from 57 to 40°C, suggesting a softening that resulted from the hydrogen bonds breaking. A thermal curing of maleimide groups was observed at about 230–260°C. Mechanical properties were also affected by the presence of maleimidophenyl; the storage modulus at 20°C increased from 1.68 (PVA) to 2.85 GPa (PVA modified with about 12% of maleimidophenyl groups), the Young's modulus from 1.16 to 1.86 GPa, and the tensile strength decreased from 65 to 57 MPa.

Eq. (27)



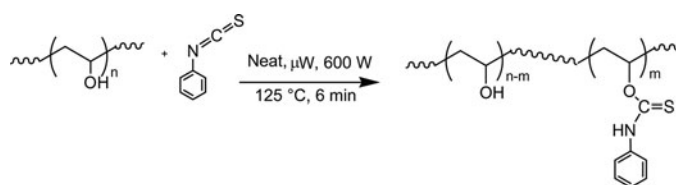
Moreno and et al.<sup>[137]</sup> introduced isocyanate function on PVA by means of a urethane linkage to end up with a novel additive for lubricants. To do so, the protection of a number of hydroxyl groups of PVA (MW = 9–10 kDa, Hy = 80%) was imposed via pyranilation with 3,4-dihydro-2-*H*-pyran (with a degree of pyranilation of about 45%), and the remaining hydroxyl groups were allowed to react with hexamethylenediisocyanate in DMF and in the presence of DBTL as catalyst, for 12 h at room temperature (Eq. 28). The highest degree of urethanation achieved was about 70%, and the ensued functionalized PVA was thermally stable up to 325°C. The measured rheological properties of the lubricant formulation using this pyranilated-isocyanated PVA as additive were enhanced.

Eq. (28)



Poly(vinyl alcohol) underwent also modification by reaction with phenyl isothiocyanate<sup>[138]</sup>, resulting in copolymer of vinyl alcohol and vinyl phenylthionecarbamate. The feature of this undertaking was that the reaction was microwave assisted (600 W and 2.45 GHz) and solvent free, and was accomplished in 6 min at 125°C (Eq. 29). The conventional procedure, that is the reaction in organic solvent at 170°C for 15 min, was disadvantaged by several flaws namely the readiness of the phenyl isothiocyanate to hydrolysis to give 1,3-diphenylthiourea (via Wohler-like reaction), and the insolubility of the copolymer obtained in organic solvents. In the environmentally friendly conditions, the yield was about 42% and the degree of functionalization was 60%.

Eq. (29)



Carbamation of PVA with octyl isocyanate in tri-*n*-butylphosphonium diethylphosphate (TBEP-DEP) was straightforward as a reaction time for quantitative modification was longer (2 days at 90°C) and required the use of a catalyst (DBTL)<sup>[121]</sup>. The urethanation in BMIM-Cl, however, seemed not to occur. Such difference in reaction behavior was linked to the capacity of the surface tension lowering of the modifying agent/ionic liquid/PVA solution.

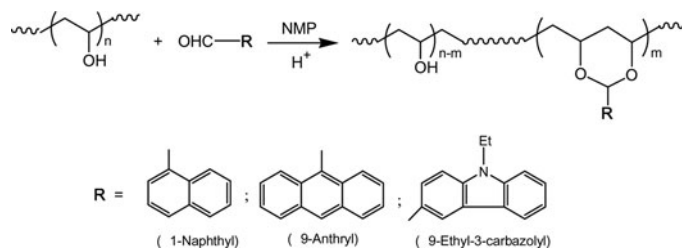
### Functionalization Through Ether Linkage

Poly(vinyl alcohol) can be modified by setting ether and silyl ether groups via its hydroxyl groups. One way to incorporate an ether functionality is through the reaction of the latter hydroxyl groups with an epoxy group-containing functionalizing agent, leading to an oxirane opening. To bring about some hydrophobic character to PVA and to improve its surface activity, Wang and his co-workers<sup>[139]</sup> undertook the quaternization with a series of glycidyl-*N*-alkyl-*N,N*-dimethylammonium chloride having fatty alkyl groups of different lengths (octyl, dodecyl, hexadecyl, octadecyl) (See Eq. (21) above). The grafting extent ranged between 6.23 and 9.96%. Mechanical results showed that the increase in grafting ratio led to a PVA toughening. The elongation at break was ~495% for PVA quaternized with 9.96% of glycidyl-*N*-dodecyl-*N,N*-dimethylammonium and that of innate PVA was lower than 50%. The  $T_g$  decreased with the alkyl chain length, from 64°C for unfunctionalized PVA to 35.18°C for quaternized PVA with glycidyl-*N*-octadecyl-*N,N*-dimethylammonium. However, the  $T_m$  and  $T_c$  (crystallization temperature) of the quaternized PVAs were higher than those for

PVA and remained almost independent of the chain length: 231 and  $\sim 206^\circ\text{C}$ , respectively, for quaternized PVAs against  $\sim 224.5$  and  $185.2^\circ\text{C}$  for PVA. The surface tensions, an indirect measure of hydrophobicity–hydrophilicity balance, of the aqueous solutions of the quaternized PVAs were in the range of  $55\text{ mN m}^{-1}$ , a value lower than that of PVA solution ( $\sim 70\text{ mN m}^{-1}$ ) at higher polymer concentrations.

The propensity of alcohol to react with aldehyde, affording acetal functionality, has been widely exploited in PVA cross-linking with a dialdehyde molecule such as glutaraldehyde, nowadays for preparing PVA-based hydrogels. Fernández et al.<sup>[140]</sup> addressed the feasibility of making poly(vinyl acetals) that contain electron-donating groups by modification of PVA (MW = 108 kDa, Hy = 98.8%) in homogeneous system using *N*-methyl-2-pyrrolidone as solvent. The monoaldehydes studied were 1-naphthaldehyde, 9-anthraldehyde, 9-ethyl-3-carbazolecarboxaldehyde and the modification reactions were run at  $40^\circ\text{C}$  for 3–7 h in the presence of Brønsted acid to catalyze the condensations (Eq. 30). Optimal reaction conditions yielded moderate acetalization degrees, 45–57%; the acetalization degree with 1-naphthaldehyde reached 81% when the reaction time was prolonged to 4 days, at a temperature of  $60^\circ\text{C}$  and with the use of an excess of aldehyde. The glass transition temperatures of acetalized PVAs increased almost linearly with increasing degree of acetalization. While the acetalization of PVA with 1-naphthaldehyde and 9-ethyl-3-carbazolecarboxaldehyde did not alter significantly the thermal stability of the pristine PVA, that with 9-anthraldehyde did but adversely.

Eq. (30)



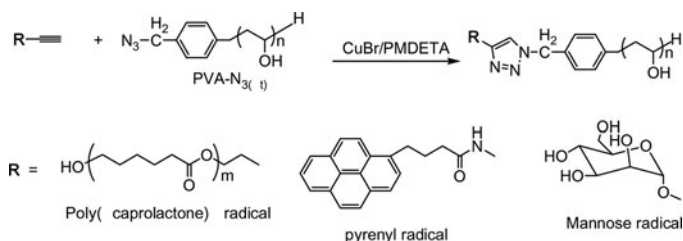
Delattre et al.<sup>[141]</sup> undertook a thorough study of acetalization of PVA of different MW's and Hy's with a number of aldehydes, including aromatics (benzaldehyde and naphthaldehyde and their derivatives) and aliphatics (decanal, undecanal and octanal and their derivatives) in the presence of *p*-toluenesulfonic acid. All prepared poly(acetal)s were obtained in moderate to high yields and were soluble in THF and other polar organic solvents. The acetalization extent with benzaldehyde was solvent and temperature dependent; the optimal functionalization was in the range of 72% either in DMSO or acetonitrile (MeCN) or in DMSO/MeCN system at  $60^\circ\text{C}$  for 1 h. The effect of the nature of the substituent in

the benzene ring on the functionalization was clear; the electron-withdrawing groups enhanced it and the electron-donating ones depressed it. Among the aliphatic aldehydes that afforded high acetalization (68–80%) were decanal, undecanal, 2-methyl-undecanal, octyl-dodecanal, and 3,7-dimethyl-octanal. Also, the modification degree was 68% for 1-naphthaldehyde and 80% for 2-naphthaldehyde and phenylacetaldehyde. While high acetalization was not hampered by high molecular weight of the pristine PVA but it was by the hydrolysis degree; PVAs with 15 to 20% of residual acetate groups could be fully functionalized, whereas those with Hy > 90% could not be acetalized. Some of these poly(acetals) could be viewed as additives in some cosmetic formulations such as nail polish and lipstick, as they provide some glossy property. Indeed, glossy measurements put those bearing naphthyl groups in front.

### Functionalization via Click Chemistry

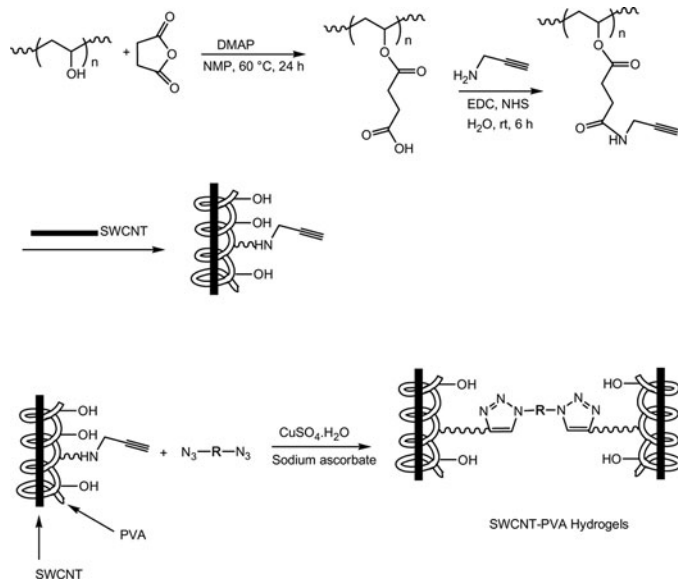
PVA with terminal azide groups (PVA- $\text{N}_{3(t)}$ ) was made by hydrolysis of poly(vinyl acetate), obtained from xanthate-mediated RAFT polymerization of vinyl acetate using *S*-(4-azidomethylbenzyl)-*O*-(2-methoxyethyl) xanthate<sup>[142]</sup>. PVA- $\text{N}_{3(t)}$  was functionalized with pyrene, poly(caprolactone), and mannose via click chemistry as illustrated in Eq. (31). The pyrene-tethered PVA displayed the fluorescent properties of pyrene molecule.

Eq. (31)



Click chemistry was used as a means of cross-linking in ensuing PVA-based hydrogel formation<sup>[143]</sup>. The strategy was to incorporate the alkyne functionality onto PVA (MW = 13–23 kDa, Hy = 87–89%) via carboxylation with succinic anhydride, and the alkynylated PVA was dispersed with single-walled carbon nanotubes (SWCNT) in DMSO, (Eq. 32). The alkynylated PVA/SWCNT hybrids were cross-linked under click chemistry with hydrophilic and hydrophobic diazides: 1,2-bis(2-azidoethoxy)ethane, 1,4-bis(azidomethyl) benzene, and 4,4'-bis(azidomethyl)-1,1'-biphenyl. Electropolymerization of 3,4-ethylenedioxythiophene occurred more efficiently in PVA/SWCNT hydrogels formed with the hydrophilic 1,2-bis(2-azidoethoxy)ethane, owing to the improvement of electrical conductivity by the SWCNTs.

Eq. (32)

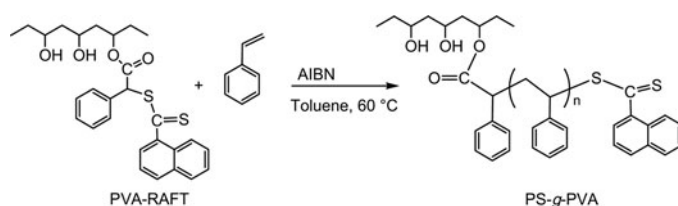


### Polymeric Grafting on PVA

Not only PVA has been functionalized with low molecular weight compounds but also with high molecular weight ones, including polymers, oligomers, and macromolecules in general. Some of this type of functionalized PVAs is appropriately cited above.

Utilization of RAFT polymerization (RAFT) allowed the grafting of polystyrene onto PVA matrix<sup>[144]</sup>. PVA (MW = 72 kDa, Hy = 98%) was esterification with 2-chloro-2-phenylacetyl chloride, followed by reaction with a Grignard reagent magnesium bromide naphthalene-1-carbodithioate to afford PVA-RAFT and subsequent RAFT strategy was applied as shown in Eq. (33). An optimal grafting ratio of 36% was achieved after a polymerization time of 48 h for a [styrene]:[PVA-RAFT] molar ratio of 500. The grafted polystyrene was of a molecular weight of MW = 26 kDa and a polydispersity index PDI of 1.6. XRD analysis confirmed the reducing effect of grafted polystyrene on the crystallinity of PVA by disruption of its intermolecular hydrogen bonding.

Eq. (33)



Graft copolymer of PVA and poly(lactic acid) was made by polymerizing L-lactic acid (LLA) or lactide in the presence

of PVA (MW = 86 kDa, Hy = 99%) in ethyl acetate using stannous 2-ethyl hexanoate as catalyst at 120 °C for 24 h (Eq. 34)<sup>[145]</sup>. Quantitative yields, up to 95%, were reached. Copolymers with less than 50 wt% of LLA showed a  $T_g$  in the range of 78 °C, approaching that of PVA (78.5 °C), but those with higher LLA content were of lower  $T_g$ s, 22–59 °C. Their  $T_m$ s were 217–228 °C, lower than that of PVA. The tensile strength, the elongation at break, and the Young's modulus of the graft copolymer varied with lactic acid content but nonsystematically; for 66 wt% content, they were 30.3 MPa, 191.4%, and 892.9 MPa, respectively. To make a hydrogel based on this graft copolymer, the grafting reaction was run in DMF/toluene and at 150 °C, a critical temperature for the hydrogel formation. The different inherent hydrogel factors were drawn from dynamic swelling measurements in water and for the hydrogel PLLA-g-PVA with 66 wt% of LLA they were as: 2.55 in swelling ratio, 0.502 in transport exponent,  $2.10 \times 10^{-7} \text{ cm}^2 \text{ s}^{-1}$  in diffusion coefficient; the value of the transport exponent hinted at a Fickian diffusion, and that of diffusion coefficient was lower than the one for PVA hydrogel. In the same year, Wang and his group<sup>[146]</sup> reported the grafting of poly(lactic acid) on PVA (DP = 1700, Hy = 99%) by conducting the graft polyesterification in melt in the presence of  $\text{SnCl}_2 \cdot \text{H}_2\text{O}$  as catalyst. The following parameters were obtained at a temperature of 95 °C, for a reaction time of 6 h, and for a catalyst concentration of 0.5 wt%: degree of substitution (DS) of 60%, degree of polymerization (DP) of grafted PLA of 1.86. The  $T_g$  and  $T_m$  were measured as 64.4, and 219 °C, respectively, values lower than those of PVA (81 and 230 °C), which may have resulted from the breaking of the hydrogen bonding of PVA, giving rise to a higher mobility. The mechanical properties were 10.6 MPa (tensile strength) and 266% (elongation at break), compared to those of the functionalized PVA were 75 MPa and 5%. These results would suggest that the oligo-PLLA grafts served as internal plasticizer for PVA polymer. The graft copolymer with DS of 60% and DP of 1.86 was partially soluble in water at 100 °C and insoluble at lower temperatures, and its water resistance was high implying its good use in food packaging. The oligo-PLLA chains reduced the hydrophilicity of PVA. Later, the same group<sup>[147]</sup> extended their investigation on the effect of oligomers of LLA on the rheological behavior of PVA. To this end, a mixture of a 1:1 blend of two types of PVA (MW = 1.7 kDa, Hy = 99%; MW = 0.5 kDa, Hy = 88%) and L-lactic acid was subjected to melt polyesterification using  $\text{SnCl}_2 \cdot \text{H}_2\text{O}$  as catalyst, affording copolymers of PVA and LLA. The degree of grafting could attain 29% and the DP of PLLA oligomers was in the range of 1.90. Besides the impact of the molecular weight of PVA, the PLLA grafting led to a melt viscosity lowering, a rise in non-Newtonian or flow index ( $n$ ) and viscous flow activation energy and, overall, an enhancement of the melting flow processing. The flow index ( $n$ ) ranged between 0.24 and 0.40 at 160 °C, and decreased with increasing of PLLA grafting.



Eq. (34)

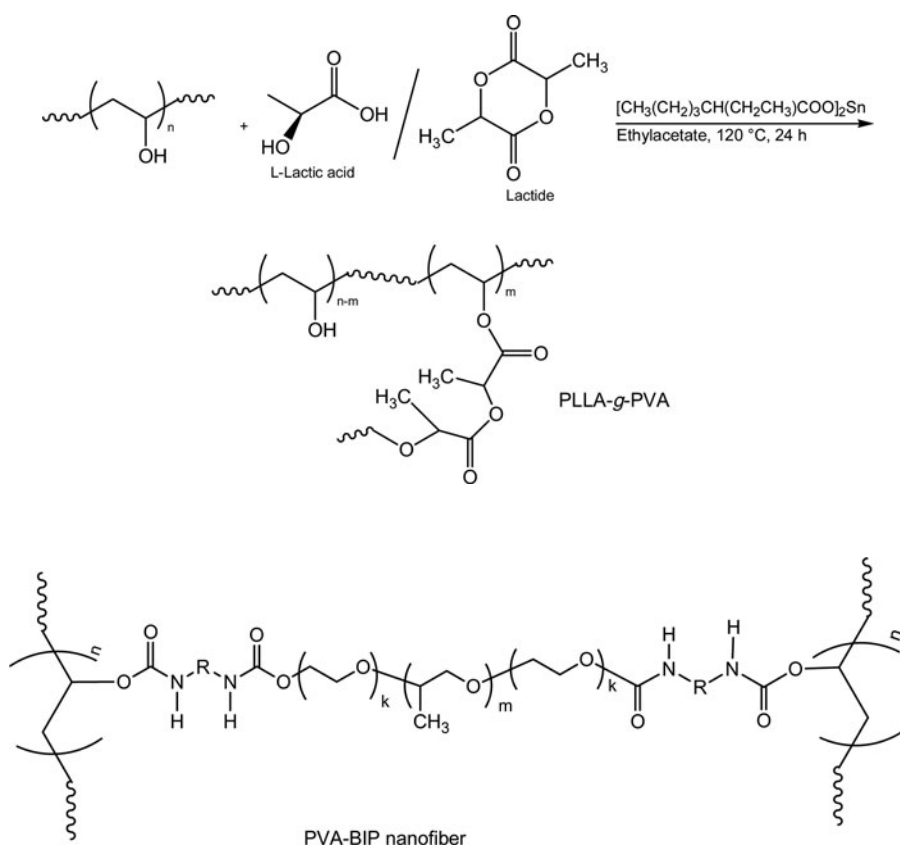


FIG. 15. PVA grafted with blocked isocyanate prepolymer. Note: PVA, poly(vinyl alcohol).

Poly(vinyl alcohol) (MW = 13–23 kDa, Hy = 88%) was grafted on chemically activated surface of low density polyethylene (LDPE) via esterification reaction at  $140^\circ C$  for 2 h<sup>[148]</sup>. The LDPE surface was activated with chromic oxide or maleic anhydride grafting, affording carboxylic acid and succinic anhydride that promoted the esterification with PVA. PVA layers were esterified in turn with poly(acrylic acid), giving rise to a ultra-thin layer on hydrophobic surface.

Poly(vinyl alcohol) (MW = 85–124 kDa, Hy = 87–89%) was affixed to polyurethane (Fig. 15) by reacting with blocked isocyanate prepolymer (BIP) in the presence of bismuth carboxylate as catalyst, using electrospinning technique to yield nanofiber mats after curing at  $170^\circ C$  for 2 min<sup>[149]</sup>. The thermal parameters,  $T_g$ ,  $T_m$ , and  $T_c$ , for PVA–BIP with 8 wt% of BIP were  $\sim 187$ ,  $\sim 71$ , and  $\sim 139^\circ C$ , respectively, against  $\sim 193$ ,  $70.8$ , and  $\sim 110^\circ C$  for the innate PVA. The cross-linked PVA–BIP nanofibers presented resistance to water, stemming from hydrophobic nature of BIP chains, as revealed by the greater contact angle  $\theta$ ; the latter angle was  $15^\circ$  and  $113^\circ$  for uncross-linked and cross-linked PVA–BIP nanofibers, respectively. The mechanical properties, Young's modulus, tensile strength, and elongation at break, were  $\sim 450$  MPa,  $\sim 54$  MPa, and 108%, respectively, for cross-linked

PVA–BIP nanofiber with 8 wt% BIP, and  $\sim 127$  MPa,  $\sim 8$  MPa, and 153% for the electrospun pristine PVA.

## CONCLUSION

In the light of the above survey on the functionalization of PVA and its link with the tailored applications, hope for a better life is optimistically held, as the research provides novel outlook to the advancement in medicine, and new hints and clues for solving problems related to the vital matters such as water. Such undertakings are in parallel with the primary concerns for researchers to ensure safety and welfare of the human beings. It appears that, to realize a useful material with a definite application, all sciences from chemistry to biology are synergistically required; hence, the research group might be multi-disciplinary. Novelties in chemistry such as the activation of hydroxyl groups with DCC, CDI, and the click chemistry, have positively served for better functionalization of PVA and novelties in techniques such as electrospinning and sol–gel have allowed preparing the functionalized PVAs for the claimed applications. An overall feeling through this review is that the chemical modification of polymers remains one of the best alternatives in working out several research-related hurdles.



## REFERENCES

- Hawker, C.J.; Wooley, K.L. The convergence of synthetic organic and polymer chemistries. *Science* **2005**, *309*, 1200–1205.
- Shahinpoor, M.; Bar-Cohen, Y.; Simpson, J.O.; Smith, J. Ionic polymer-metal composites (IPMCs) as biomimetic sensors, actuators and artificial muscles – A review. *Smart Mater. Struct.* **1998**, *7*, R15–R30.
- Harsányi, G. Polymer films in sensor applications: A review of present uses and future possibilities. *Sensor Rev.* **2000**, *20*, 98–105.
- Schmaljohann, D. Thermo- and pH-responsive polymers in drug delivery. *Adv. Drug Deliv. Rev.* **2006**, *58*, 1655–1670.
- Mehdizadeh, M.; Weng, H.; Gyawali, D.; Tang, L.; Yang, J. Injectable citrate-based mussel-inspired tissue bioadhesives with high wet strength for sutureless wound closure. *Biomaterials* **2012**, *33*, 7972–7983.
- Spanggaard, H.; Krebs, F.C. A brief history of the development of organic and polymeric photovoltaics. *Sol. Energy Mater. Sol. Cells* **2004**, *83*, 125–146.
- Chen, J.; Cao, Y. Development of novel conjugated donor polymers for high-efficiency bulk-heterojunction photovoltaic devices. *Acc. Chem. Res.* **2009**, *42*, 1709–1718.
- Shuttleworth, S.J.; Allin, M.; Sharma, P.K. Functionalised polymers: Recent developments and new applications in synthetic organic chemistry. *Synthesis* **1997**, *11*, 1217–1239.
- Lu, J.; Toy, P.H. Organic polymer supports for synthesis and for reagent and catalyst immobilization. *Chem. Rev.* **2009**, *109*, 815–838.
- Finch, C.A. ed., *Polyvinyl Alcohol, Properties and Applications*, Wiley, London, 1973.
- Finch, C.A. *Polyvinyl Alcohol, Developments*, Wiley, New York, 1992.
- Moulay, S. Poly(vinyl alcohol): What a material! what a chemistry! In: Pandalai, S.G., ed. *Recent Research and Developments in Applied Polymer Science*, Research Signpost: Kerala, India, 2009, Vol. 4, Part II, pp. 391–496.
- Smith, A.A.A.; Hussmann, T.; Elich, J.; Postma, A.; Alvesa, M.-H.; Zelikin, A.N. Macromolecular design of poly(vinyl alcohol) by RAFT polymerization. *Polym. Chem.* **2012**, *3*, 85–88.
- Siskin, G.P.; Englander, M.; Stainken, B.F.; Ahn, J.; Dowling, K.; Dolen, E.G. Embolic agents used for uterine fibroid embolization. *Am. J. Roentgenol.* **2000**, *175*, 767–773.
- Baker, M.; Walsh, S.P.; Schwartz, Z.; Boyan, B.D. A review of polyvinyl alcohol and its uses in cartilage and orthopedic applications. *J. Biomed. Mater. Res. Part B: Appl. Biomater.* **2012**, *100B*(5), 1451–1457.
- Kobayashi, M. Development and evaluation of poly(vinyl alcohol) hydrogels as a component of hybrid artificial tissues for orthopedics surgery application, in Dumitru, S. and Popa, V., eds. *Polymeric Materials*, CRC Press, Boca Raton, 2013, Vol. 1, pp. 57–81.
- Marin, E.; Rojas, J.; Ciro, Y. A review of polyvinyl alcohol: Promising materials for pharmaceutical and biomedical applications. *African J. Pharm. Pharmacol.* **2014**, *8*, 674–684.
- Filippo, E.; Serra, A.; Manno, D. Poly(vinyl alcohol) capped silver nanoparticles as localized surface plasmon resonance-based hydrogen peroxide sensor. *Sens. Actuators, B* **2009**, *138*, 625–630.
- Galya, T.; Sedlářík, V.; Kuřitka, I.; Novotný, R.; Sedlářková, J.; Sába, P. Antibacterial poly(vinyl alcohol) film containing silver nanoparticles: Preparation and characterization. *J. Appl. Polym. Sci.* **2008**, *110*, 3178–3185.
- Son, B.; Yeom, B.-Y.; Song, S.H.; Lee, C.-S.; Hwang, T.S. Antibacterial electrospun chitosan/poly(vinyl alcohol) nanofibers containing silver nitrate and titanium dioxide. *J. Appl. Polym. Sci.*, **2009**, *111*, 2892–2899.
- Bryaskova, R.; Pencheva, D.; Kyulavska, M.; Bozukova, D.; Debuigne, A.; Detrembleur, C. Antibacterial activity of poly(vinyl alcohol)-*b*-poly(acrylonitrile) based micelles loaded with silver nanoparticles. *J. Colloid Interf. Sci.* **2010**, *344*, 424–428.
- Banerjee, M.; Sachdev, P.; Mukherjee, G.S. Preparation of PVA/Co/Ag film and evaluation of its magnetic and microstructural properties. *J. Appl. Phys.* **2012**, *111*, 094302.
- Mahanta, N.; Valiyaveetil, S. Functionalized poly(vinyl alcohol) based nanofibers for the removal of arsenic from water. *RSC Adv.* **2013**, *3*, 2776–2783.
- Salunkhe, A.B.; Khot, V.M.; Thorat, N.D.; Phadate, M.R.; Sathish, C. I.; Dhawale, D.S.; Pawar, S.H. Polyvinyl alcohol functionalized cobalt ferrite nanoparticles for biomedical applications. *Appl. Surf. Sci.* **2013**, *264*, 598–604.
- Maruyama, H.; Moritani, T.; Akazawa, T.; Sato, T. New modifications of poly(vinyl alcohol)s and their applications, *British Polym. J.* **1988**, *20*, 345–351.
- Wang, Y.; Chen, K.S.; Mishler, J.; Cho, S.C.; Adroher, X.C. A review of polymer electrolyte membrane fuel cells: Technology, applications, and needs on fundamental research. *Appl. Energy* **2011**, *88*, 981–1007.
- Gu, S.; He, G.; Wu, X.; Guo, Y.; Liu, H.; Peng, L.; Xiao, G. Preparation and characteristics of crosslinked sulfonated poly(phthalazinone ether sulfone ketone) with poly(vinyl alcohol) for proton exchange membrane. *J. Membr. Sci.*, **2008**, *312*, 48–58.
- Mollá, S.; Compañ, V. Polyvinyl alcohol nanofiber reinforced Nafion membranes for fuel cell applications. *J. Membr. Sci.* **2011**, *372*, 191–200.
- Tseng, C.-Y.; Ye, Y.-S.; Kao, K.-Y.; Joseph, J.; Shen, W.-C.; Rick, J.; Hwang, B.-J. Interpenetrating network-forming sulfonated poly(vinyl alcohol) proton exchange membranes for direct methanol fuel cell applications. *Intern. J. Hydrogen Energy* **2011**, *36*, 11936–11945.
- Boroglu, M.S.; Cavus, S.; Boz, I.; Ata, A. Synthesis and characterization of poly(vinyl alcohol) proton exchange membranes modified with 4,4-diaminodiphenylether-2,2-disulfonic acid. *eXPRESS Polym. Lett.* **2011**, *5*, 470–478.
- Yun, S.; Im, H.; Heo, Y.; Kim, J. Crosslinked sulfonated poly(vinyl alcohol)/sulfonated multi-walled carbon nanotubes nanocomposite membranes for direct methanol fuel cells. *J. Membr. Sci.* **2011**, *380*, 208–215.
- Yoo, M.; Kim, M.; Hwang, Y.; Kim, J. Fabrication of highly selective PVA-g-GO/SPVA membranes via cross-linking method for direct methanol fuel cells. *Ionics* **2014**, *20*, 875–886.
- Pan, W.-H.; Lue, S.J.; Chang, C.-M.; Liu, Y.-L. Alkali doped polyvinyl alcohol/multi-walled carbon nano-tube electrolyte for direct methanol alkaline fuel cell. *J. Membr. Sci.* **2011**, *376*, 225–232.
- Lue, S.J.; Pan, W.-H.; Chang, C.-M.; Liu, Y.-L. High-performance direct methanol alkaline fuel cells using potassium hydroxide-impregnated polyvinyl alcohol/carbon nano-tube electrolytes. *J. Power Sources* **2012**, *202*, 1–10.
- Goldbach, J.T. Blend of ionic (co)polymer resins and matrix (co)polymers, *US Patent* 7, 629, 426 B2, December 8, 2009.
- Shin, M.-S.; Byun, Y.-J.; Choi, Y.-W.; Kang, M.-S.; Park, J.-S. On-site crosslinked quaternized poly(vinyl alcohol) as ionomer binder for solid alkaline fuel cells. *Int. J. Hydrogen Energy* **2014**, *39*, 16556–16561.
- Ulery, B.D.; Nair, L.S.; Laurencin, C.T. Biomedical applications of biodegradable polymers. *J. Polym. Sci. B Polym. Phys.* **2011**, *49*, 832–864.
- Lim, K.S.; Alves, M.H.; Poole-Warren, L.A.; Martens, P.J. Covalent incorporation of non-chemically modified gelatin into degradable PVA-tyramine hydrogels. *Biomaterials* **2013**, *34*, 7097–7105.
- Reis, A.V.; Fajardo, A.R.; Schuquel, I.T.A.; Guilherme, M.R.; Vidotti, G.J.; Rubira, A.F.; Muniz, E.C. Reaction of glycidyl methacrylate at the hydroxyl and carboxylic groups of poly(vinyl alcohol) and poly(acrylic acid): is this reaction mechanism still unclear? *J. Org. Chem.* **2009**, *74*, 3750–3757.
- Crispim, E.G.; Piai, J.F.; Fajardo, A.R.; Ramos, E.R.F.; Nakamura, T.U.; Nakamura, C.V.; Rubira, A.F.; Muniz, E.C. Hydrogels based on chemically modified poly(vinyl alcohol) (PVA-GMA) and PVA-GMA/chondroitin sulfate: Preparation and characterization. *eXPRESS Polym. Lett.* **2012**, *6*, 383–395.
- Kartal, F.; Akkaya, A.; Kilinc, A. Immobilization of porcine pancreatic lipase on glycidyl methacrylate grafted polyvinyl alcohol. *J. Mol. Catal. B: Enzym.* **2009**, *57*, 55–61.

42. Oktay, B.; Kayaman-Apohan, N.; Erdem-Kuruca, S. Fabrication of Nanofiber Mats from Electrospinning of Functionalized Polymers, IOP Conf. Series, 2nd International Conference on Structural Nano Composites (NANOSTRUC 2014), Consejo Superior de Investigaciones Científicas (CSIC), Calle de Serrano 123, 28006, Madrid, Spain, Materials Science and Engineering, 64, 012011, 2014.
43. Bader, R.A. Synthesis and viscoelastic characterization of novel hydrogels generated via photopolymerization of 1,2-epoxy-5-hexene modified poly(vinyl alcohol) for use in tissue replacement. *Acta Biomater.* **2008**, *4*, 967–975.
44. Wang, C.-C.; Yang, F.-L.; Liu, L.-F.; Fu, Z.-M.; Xue, Y. Hydrophilic and antibacterial properties of polyvinyl alcohol/4-vinylpyridine graft polymer modified polypropylene non-woven fabric membranes. *J. Membr. Sci.* **2009**, *345*, 223–232.
45. Wang, C.; Yang, F.; Duan, J.; Zhang, H. Nonwoven membrane modification by 4-vinylpyridine grafted polyvinyl alcohol for resistance the adhesion of bacteria. *Desalin. Water Treat.* **2010**, *18*, 206–211.
46. Blum, M.M.; Ovaert, T.C. A novel polyvinyl alcohol hydrogel functionalized with organic boundary lubricant for use as low-friction cartilage substitute: Synthesis, physical/chemical, mechanical, and friction characterization. *J. Biomed. Mater. Res., Part B* **2012**, *100B*, 1755–1763.
47. Blum, M.M.; Ovaert, T.C. Investigation of friction and surface degradation of innovative boundary lubricant functionalized hydrogel material for use as artificial articular cartilage. *Wear* **2013**, *301*, 201–209.
48. Ossipov, D.A.; Hilborn, J. Versatile functionalization of poly(vinyl alcohol) for grafting of biofunctional building blocks. *Polym. Prepr.* **2007**, *48*, 182–183.
49. Alves, M.H.; Young, C.J.; Bozzetto, K.; Poole-Warren, L.A.; Martens, P.J. Degradable, click poly(vinyl alcohol) hydrogels: Characterization of degradation and cellular compatibility. *Biomed. Mater.* **2012**, *7*, 024106.
50. Montalbetti, C.A.G.N.; Falque, V. Amide bond formation and peptide coupling. *Tetrahedron* **2005**, *61*, 10827–10852.
51. Rafat, M.; Rotenstein, L.S.; You, J.-O.; Auguste, D.T. Dual functionalized PVA hydrogels that adhere endothelial cells synergistically. *Biomaterials* **2012**, *33*, 3880–3886.
52. Millon, L.E.; Padavan, D.T.; Hamilton, A.M.; Boughner, D.R.; Wan, W. Exploring cell compatibility of a fibronectin-functionalized physically crosslinked poly(vinyl alcohol) hydrogel. *J. Biomed. Mater. Res. B: Appl. Biomater.* **2012**, *100B*, 1–10.
53. Sun, P.; Chen, J.; Liu, Z.-W.; Liu, Z.-T. Poly(vinyl alcohol) functionalized  $\beta$ -cyclodextrin as an inclusion complex. *J. Macromol. Sci. Part A* **2009**, *46*, 533–540.
54. Lee, M.S.; Kim, J.-C.  $\beta$ -Cyclodextrin/poly(vinyl alcohol) hydrogels containing phenylpropionic acid and naphthylamine: Dual pH-sensitive release. *Polym. Int.* **2014**, *63*, 989–996.
55. Lee, M.S.; Kim, J.-C. Photo-responsive monoolein cubic phase incorporating hydrophobically modified poly(vinyl alcohol)-coumarin conjugate. *Polym. Eng. Sci.*, **2014**, *54*, 227–233.
56. Seo, H.J.; Cha, H.J.; Kim, T.S.; Kim, J.-C. Photo-responsive liposomes decorated with hydrophobically modified poly(vinyl alcohol)-coumarin conjugate. *J. Ind. Eng. Chem.* **2013**, *19*, 310–315.
57. Wang, B.; Guan, X.; Hu, Y.; Su, Z. Preparation and fluorescent properties of poly(vinyl alcohol) bearing coumarin. *Polym. Adv. Technol.* **2007**, *18*, 529–534.
58. Lee, M.S.; Kim, J.-C. Photodependent release from poly(vinyl alcohol)/epoxypropoxy coumarin hydrogels. *J. Appl. Polym. Sci.* **2012**, *124*(5) 4339–4345.
59. Lee, M.S.; Mok, E.Y.; Shin, W.C.; Kim, J.D.; Kim, J.-C. Poly(vinyl alcohol) hollow microcapsules prepared by emulsification, salting out, and photo cross-linking method. *Korean J. Chem. Eng.* **2012**, *29*, 1108–1113.
60. Zan, X.; Kozlov, M.; McCarthy, T.J.; Su, Z. Covalently attached, silver-doped poly(vinyl alcohol) hydrogel films on poly(L-lactic acid). *Biomacromolecules* **2010**, *11*, 1082–1088.
61. Nafea, E.H.; Poole-Warren, L.A.; Martens, P.J. Structural and functional characterization of biosynthetic PVA-gelatin hydrogels designed for cell based therapy, In: Long, M. ed. *World Congress on Medical Physics and Biomedical Engineering, IFMBE Proceedings*, Heidelberg, Germany. Vol. 39, pp. 91–94, 2013.
62. Holloway, J.L.; Lowman, A.M.; VanLandingham, M.R.; Palmese, G.R. Chemical grafting for improved interfacial shear strength in UHMWPE/PVA-hydrogel fiber-based composites used as soft fibrous tissue replacements. *Compos. Sci. Technol.* **2013**, *85*, 118–125.
63. Kupal, S.G.; Cerroni, B.; Ghugare, S.V.; Chiessi, E.; Paradossi, G. Biointerface properties of core-shell poly(vinyl alcohol)-hyaluronic acid microgels based on chemoselective chemistry. *Biomacromolecules* **2012**, *13*, 3592–3601.
64. Xu, L.; Li, Y.; Li, Y. Application of “click” chemistry to the construction of supramolecular functional systems. *Asian J. Org. Chem.* **2014**, *3*, 582–602.
65. Gacal, B.N.; Koz, B.; Gacal, B.; Kiskan, B.; Erdogan, M.; Yagci, Y. Pyrene functional poly(vinyl alcohol) by “click” chemistry. *J. Polym. Sci. Part A: Polym. Chem.* **2009**, *47*, 1317–1326.
66. Odaci, D.; Gacal, B.N.; Gacal, B.; Timur, S.; Yagci, Y. Fluorescence sensing of glucose using glucose oxidase modified by PVA-pyrene prepared via “click” chemistry. *Biomacromolecules* **2009**, *10*, 2928–2934.
67. Medine, E.I.; Odaci, D.; Gacal, B.N.; Gacal, B.; Sakarya, S.; Unak, P.; Timur, S.; Yagci, Y. A new approach for in vitro imaging of breast cancer cells by anti-metadherin targeted PVA-pyrene. *Macromol. Biosci.* **2010**, *10*, 657–663.
68. Cui, Q.; Hou, Y.; Hou, J.; Pan, P.; Li, L.-Y.; Bai, G.; Luo, G. Preparation of functionalized alkynyl magnetic microspheres for the selective enrichment of cell glycoproteins based on click chemistry. *Biomacromolecules* **2013**, *14*, 124–131.
69. Huang, J.; Wang, D.; Lu, Y.; Li, M.; Xu, W. Surface zwitterionically functionalized PVA-co-PE nanofiber materials by click chemistry. *RSC Adv.* **2013**, *3*, 20922–20929.
70. Jantas, R.; Draczyński, Z.; Herczyńska, L.; Stawski, D. Poly(vinyl alcohol)-salicylic acid conjugate: Synthesis and characterization, *Am. J. Polym. Sci.* **2012**, *2*, 79–84.
71. Cristescu, R.; Popescu, C.; Popescu, A.C.; Grigorescu, S.; Duta, L.; Mihailescu, I.N.; Caraene, G.; Albuiescu, R.; Albuiescu, L.; Andronic, A.; Stamatin, I.; Ionescu, A.; Mihaiescu, D.; Buruiana, T.; Chrissey, D. B. Functionalized polyvinyl alcohol derivatives thin films for controlled drug release and targeting systems: MAPLE deposition and morphological, chemical and in vitro characterization. *Appl. Surf. Sci.* **2009**, *255*, 5600–5604.
72. Sun, Z.C.; Wei, Z.; Wei, K.M. Preparation of aldehyde-, amino-, and hydrazide-functionalized polymer particles for direct immobilization of the sugars. *J. Appl. Polym. Sci.* **2009**, *114*, 2937–2945.
73. Kenawy, E.-R.; El-Newehy, M.H.; Abdel-Hay, F.I.; El-Shanshoury, A.R. Synthesis and biocidal activity of modified poly(vinyl alcohol). *Arabian J. Chem.* **2014**, *7*, 355–361.
74. Ma, B.; Zeng, F.; Zhenga, F.; Wu, S. Fluorescent detection of an anthrax biomarker based on PVA film. *Analyst* **2011**, *136*, 3649–3655.
75. Sahoo, N.G.; Bao, H.; Pan, Y.; Pal, M.; Kakran, M.; Cheng, H.K.F.; Li, L.; Tan, L.P. Functionalized carbon nanomaterials as nanocarriers for loading and delivery of a poorly water-soluble anticancer drug: A comparative study. *Chem. Commun.* **2011**, *47*, 5235–5237.
76. Kakran, M.; Li, L. Carbon nanomaterials for drug delivery. *Key Eng. Mater.* **2012**, *508*, 76–80.
77. Hurtgen, M.; Debuigne, A.; Hoebeke, M.; Passirani, C.; Lautram, N.; Mouithys-Mickalad, A.; Guelluy, P.-H.; Jérôme, C.; Detrembleur, C. Photochemical properties and activity of water-soluble polymer/C<sub>60</sub> nano-hybrids for photodynamic therapy. *Macromol. Biosci.* **2013**, *13*, 106–115.
78. Cavusoglu, J.; Kusefoglu, S.H. Oleophilic modification of poly(vinyl alcohol) films by functionalized soybean oil triglycerides. *J. Appl. Polym. Sci.* **2011**, *119*, 2431–2438.

79. Kaneko, Y.; Matsuda, S.-i.; Kadokawa, J.-i. Chemoenzymatic synthesis of amylose-grafted poly(vinyl alcohol). *Polym. Chem.* **2010**, *1*, 193–197.
80. Mahanta, N.; Valiyaveetil, S. Surface modified electrospun poly(vinyl alcohol) membranes for extracting nanoparticles from water. *Nanoscale* **2011**, *3*, 4625–4631.
81. Xiong, W.; Guan, Y.; Guo, C.; Yang, M.; Xia, T.; Zhao, S. Preparation of thiourea functionalized polyvinyl alcohol-coated magnetic nanoparticles and their application in  $Pb^{2+}$  ions adsorption. *J. Appl. Polym. Sci.* **2014**, *131*, 40777. doi:10.1002/APP.40777
82. Wu, S.; Li, F.; Wang, H.; Fu, L.; Zhang, B.; Li, G. Effects of poly(vinyl alcohol) (PVA) content on preparation of novel thiol-functionalized mesoporous PVA/SiO<sub>2</sub> composite nanofiber membranes and their application for adsorption of heavy metal ions from aqueous solution. *Polymer* **2010**, *51*, 6203–6211.
83. Wu, S.; Li, F.; Wu, Y.; Xu, R.; Li, G. Preparation of novel poly(vinyl alcohol)/SiO<sub>2</sub> composite nanofiber membranes with mesostructure and their application for removal of  $Cu^{2+}$  from waste water. *Chem. Commun.* **2010**, *46*, 1694–1696.
84. Irani, M.; Keshkar, A.R.; Mousavian, M.A. Removal of Cd(II) and Ni(II) from aqueous solution by PVA/TEOS/TMPTMS hybrid membrane. *Chem. Eng. J.* **2011**, *175*, 251–259.
85. Irani, M.; Keshkar, A.R.; Mousavian, M.A. Removal of cadmium from aqueous solution using mesoporous PVA/TEOS/APTES composite nanofiber prepared by sol-gel/electrospinning. *Chem. Eng. J.* **2012**, *200–202*, 192–201.
86. Keshkar, A.R.; Irani, M.; Mousavian, M.A. Comparative study on PVA/silica membrane functionalized with mercapto and amine groups for adsorption of Cu(II) from aqueous solutions. *J. Taiwan Inst. Chem. Eng.* **2013**, *44*, 279–286.
87. Nasir, S.M.; Nur, H. Gold nanoparticles embedded on the surface of polyvinyl alcohol layer. *J. Fundam. Sci.* **2008**, *4*, 245–252.
88. Chi, F.; Wang, X.; Xiong, J.; Hu, S. Polyvinyl alcohol fibers with functional phosphonic acid group: synthesis and adsorption of uranyl (VI) ions in aqueous solutions. *J. Radioanal. Nucl. Chem.* **2013**, *296*, 1331–1340.
89. Karpagam, S.; Thangaraj, R.; Guhanathan, S. Functional modification of poly(vinyl alcohol) through phosphorus containing nitrogen heterocyclic moieties. *J. Appl. Polym. Sci.* **2008**, *110*, 2549–2554.
90. Karpagam, S.; Guhanathan, S. Flame-retardant and morphological analysis of nitrogen heterocycle-modified poly(vinyl alcohol) and their application for adsorption of heavy metal ions. *J. Appl. Polym. Sci.* **2013**, *129*, 2046–2056.
91. Abdel-Razik, H.H.; Abbo, M.; Almahy, H.A. Polymer-based metal adsorbents via graft copolymerization of polyvinyl alcohol with diaminomaleonitrile: A green chemistry approach. *J. Appl. Polym. Sci.* **2012**, *125*, 2102–2109.
92. Liong, M.; Shao, H.; Haun, J.B.; Lee, H.; Weissleder, R. Carboxymethylated polyvinyl alcohol stabilizes doped ferrofluids for biological applications. *Adv. Mater.* **2010**, *22*, 5168–5172.
93. Ismanto, A.E.; Liu, J.C. Enhanced boron adsorption using PVA-modified carbonaceous materials. *Comp. Interf.* **2014**, *21*, 639–650.
94. Isaad, J.; Salaün, F. Functionalized poly(vinyl alcohol) polymer as chemodosimeter material for the colorimetric sensing of cyanide in pure water. *Sens. Actuators, B* **2011**, *157*, 26–33.
95. Meng, X.J.; Liu, Q.L.; Zhu, A.M.; Zhang, Q.G. Amino-functionalized poly(vinyl alcohol) membranes for enhanced water permselectivity. *J. Membr. Sci.* **2010**, *360*, 276–283.
96. Zhang, Q.G.; Liu, Q.L.; Zhu, A.M.; Xiong, Y.; Ren, L. Pervaporation performance of quaternized poly(vinyl alcohol) and its crosslinked membranes for the dehydration of ethanol. *J. Membr. Sci.* **2009**, *335*, 68–75.
97. Rachipudi, P.S.; Kariduraganavar, M.Y.; Kittur, A.A.; Sajjan, A.M. Synthesis and characterization of sulfonated-poly(vinyl alcohol) membranes for the pervaporation dehydration of isopropanol. *J. Membr. Sci.* **2011**, *383*, 224–234.
98. Shang, Y.; Peng, Y. UF membrane of PVA modified with TDI. *Desalination* **2008**, *221*, 324–330.
99. Moore, D.R.; Duong, H.M.; Hutchinson, R.A. Processes for forming permanent hydrophilic porous coating onto a substrate, and porous membranes therefor, *US Patent* 2009/0191357 A1, July 30, 2009.
100. Li, M.; Wang, H.; Wu, S.; Li, F.; Zhi, P. Adsorption of hazardous dyes indigo carmine and acid red on nanofiber membranes. *RSC Adv.* **2012**, *2*, 900–907.
101. Teng, M.; Li, F.; Zhang, B.; Taha, A.A. Electrospun cyclodextrin-functionalized mesoporous polyvinyl alcohol/SiO<sub>2</sub> nanofiber membranes as a highly efficient adsorbent for indigo carmine dye. *Colloids Surf., A* **2011**, *385*, 229–234.
102. Zhu, J.; Yang, J.; Sun, G. Cibacron blue F3GA functionalized poly(vinyl alcohol-co-ethylene) (PVA-co-PE) nanofibrous membranes as high efficient affinity adsorption materials. *J. Membr. Sci.* **2011**, *385–386*, 269–276.
103. Fatehi, P.; Xiao, H. Adsorption characteristics of cationic-modified poly(vinyl alcohol) on cellulose fibers-A qualitative analysis. *Colloids Surf., A* **2008**, *327*, 127–133.
104. Fatehi, P.; Singh, R.; Ziaee, Z.; Xiao, H.; Ni, Y. Preparation and characterization of cationic polyvinyl alcohol. *Eur. Polym. J.* **2011**, *47*, 997–1004.
105. Fatehi, P.; Tutus, A.; Xiao, H. Cationic-modified PVA as a dry strength additive for rice straw fibers. *Biores. Technol.* **2009**, *100*, 749–755.
106. Fatehi, P.; Xiao, H. Effect of cationic PVA characteristics on fiber and paper properties at saturation level of polymer adsorption. *Carbohydr. Polym.* **2010**, *79*, 423–428.
107. Kara, S.; Gacal, B.; Tunc, D.; Yagci, Y.; Pekcan, Ö. Sorption and desorption of PVA-pyrene chains in and out of agarose gel. *J. Fluoresc.* **2012**, *22*, 1073–1080.
108. Sridhar, V.; Oh, I.-K. A coagulation technique for purification of graphene sheets with graphene-reinforced PVA hydrogel as byproduct. *J. Colloid Interf. Sci.* **2010**, *348*, 384–387.
109. Xu, L.; Dong, X.-Y.; Sun, Y. Electroosmotic pump-assisted capillary electrophoresis of proteins. *J. Chromatogr. A* **2009**, *1216*, 6071–6076.
110. Xu, L.; Dong, X.-Y.; Sun, Y. Novel poly(vinyl alcohol)-based column coating for capillary electrophoresis of proteins. *Biochem. Eng. J.* **2010**, *53*, 137–142.
111. Hwang, C.-C.; Wang, L.; Lu, W.; Ruan, G.; Kini, G.C.; Xiang, C.; Samuel, E.L.G.; Shi, W.; Kan, A.T.; Wong, M.S.; Tomson, M.B.; Tour, J.M. Highly stable carbon nanoparticles designed for downhole hydrocarbon detection. *Energy Environ. Sci.*, **2012**, *5*, 8304–8309.
112. Sherrington, D.C. Polymer-supported synthesis. In: Clark, J.H. ed. *Chemistry of Waste Minimisation*, Glasgow: Blackie, 1995, Chapter 6, pp. 141–200.
113. Pito, D.S.; Fonseca, I.M.; Ramos, A.M.; Vital, J.; Castanheiro, J.E. Methoxylation of  $\alpha$ -pinene over poly(vinyl alcohol) containing sulfonic acid groups. *Chem. Eng. J.* **2009**, *147*, 302–306.
114. Caetano, C.S.; Guerreiro, L.; Fonseca, I.M.; Ramos, A.M.; Vital, J.; Castanheiro, J.E. Esterification of fatty acids to biodiesel over polymers with sulfonic acid groups. *Appl. Catal., A* **2009**, *359*, 41–46.
115. Pito, D.S.; Fonseca, I.M.; Ramos, A.M.; Vital, J.; Castanheiro, J.E. Hydrolysis of sucrose using sulfonated poly(vinyl alcohol) as catalyst. *Biores. Technol.* **2009**, *100*, 4546–4550.
116. Zucca, P.; Sollai, F.; Garau, A.; Rescigno, A.; Sanjust, E. Fe(III)-5,10,15,20-Tetrakis(pentafluorophenyl)porphine supported on pyridyl-functionalized, crosslinked poly(vinyl alcohol) as a biomimetic versatile-peroxidase-like catalyst. *J. Mol. Catal. A: Chem.* **2009**, *306*, 89–96.
117. Zucca, P.; Cocco, G.; Pintus, M.; Rescigno, A.; Sanjust, E. Biomimetic sulfide oxidation by the means of immobilized Fe(III)-5,10,15,20-tetrakis(pentafluorophenyl)porphin under mild experimental conditions. *J. Chem.* **2013**, *2013*, 1–7. Article ID 651274.
118. Casimiro, M.H.; Silva, A.G.; Pinto, J.V.; Ramos, A.M.; Vital, J.; Ferreira, L.M. Catalytic poly(vinylalcohol) functionalized membranes obtained by gamma irradiation. *Rad. Phys. Chem.* **2012**, *81*, 1314–1318.

119. Salavagione, H.J.; Martínez, G.; Gómez, R.; Segura, J.L. Synthesis of water-soluble perylene-3,4,9,10-tetracarboxylic diimide-functionalized polymer through esterification with poly(vinyl alcohol). *J. Polym. Sci. Part A: Polym. Chem.* **2010**, *48*, 3613–3622.
120. Mukherjee, G.S. Calorimetric characterization of membrane materials based on poly(vinyl alcohol). *J. Therm. Anal. Calorim.* **2009**, *96*, 21–25.
121. Eastman, S.A.; Lesser, A.J.; McCarthy, Th.J. Quantitative poly(vinyl alcohol) modification in ionic liquids: esterification and urethanation with low surface tension producing reagents. *Macromolecules* **2010**, *43*, 4584–4588.
122. Fernández, M.D.; Fernández, M.J. Cyclic ureas as solvents for esterification of poly(vinyl alcohol) and vinyl acetate-vinyl alcohol copolymers with acid chlorides. *J. Appl. Polym. Sci.* **2008**, *107*, 2509–2519.
123. Sangngern, S.; Sahasithiwat, S.; Koonsaeng, N.; Laobuthee, A. Study on chemical vapour sensing property of esterified poly(vinyl alcohol). *Adv. Mater. Res.* **2010**, *93–94*, 185–189.
124. Wang, J.; Satoh, M. Novel PVA-based polymers showing an anti-Hofmeister series property. *Polymer* **2009**, *50*, 3680–3685.
125. Mori, M.; Wang, J.; Satoh, M. Anti-Hofmeister series properties found for a polymer having a  $\pi$  electron system and acidic protons. *Colloid. Polym. Sci.* **2009**, *287*, 123–127.
126. Salavagione, H.J.; Martínez, G.; Ellis, G. Recent advances in the covalent modification of graphene with polymers. *Macromol. Rapid Commun.* **2011**, *32*, 1771–1789.
127. Zhao, X.; Zhang, Q.; Chen, D. Enhanced mechanical properties of graphene-based poly(vinyl alcohol) composites. *Macromolecules* **2010**, *43*, 2357–2363.
128. Cheng, H.K.F.; Sahoo, N.G.; Tan, Y.P.; Pan, Y.; Bao, H.; Li, L.; Chan, S.H.; Zhao, J. Poly(vinyl alcohol) nanocomposites filled with poly(vinyl alcohol)-grafted graphene oxide. *ACS Appl. Mater. Interfaces* **2012**, *4*, 2387–2394.
129. Veca, L.M.; Lu, F.; Meziani, M.J.; Cao, L.; Zhang, P.; Qi, G.; Qu, L.; Shrestha, M.; Sun, Y.-P. Polymer functionalization and solubilization of carbon nanosheets. *Chem. Commun.* **2009**, *18*, 2565–2567.
130. Wang, D.; Bao, Y.; Zha, J.-W.; Zhao, J.; Dang, Z.-M.; Hu, G.-H. Improved dielectric properties of nanocomposites based on poly(vinylidene fluoride) and poly(vinyl alcohol)-functionalized graphene. *ACS Appl. Mater. Interfaces* **2012**, *4*, 6273–6279.
131. Shen, B.; Zhai, W.; Lu, D.; Wang, J.; Zheng, W. Ultrasonication-assisted direct functionalization of graphene with macromolecules. *RSC Adv.* **2012**, *2*, 4713–4719.
132. Salavagione, H.J.; Gómez, M.A.; Martínez, G. Polymeric modification of graphene through esterification of graphite oxide and poly(vinyl alcohol). *Macromolecules* **2009**, *42*, 6331–6334.
133. Zhang, F.M.; Chang, J.; Eberhard, B. Dissolution of poly(vinyl alcohol)-modified carbon nanotubes in a buffer solution. *New Carbon Mater.* **2010**, *25*, 241–247.
134. Fu, C.; Gu, L. Composite fibers from poly(vinyl alcohol) and poly(vinyl alcohol)-functionalized multiwalled carbon nanotubes. *J. Appl. Polym. Sci.* **2013**, *128*, 1044–1053.
135. Zhao, X.; Zhang, Q.; Hao, Y.; Li, Y.; Fang, Y.; Chen, D. Alternate multilayer films of poly(vinyl alcohol) and exfoliated graphene oxide fabricated via a facial layer-by-layer assembly. *Macromolecules* **2010**, *43*, 9411–9416.
136. Gaina, C.; Ursache, O.; Gaina, V.; Ionita, D. Study on the chemical modification of poly(vinyl alcohol) with 4-maleimidophenyl isocyanate. *Polym. Plast. Technol. Eng.* **2012**, *51*, 65–70.
137. Moreno, G.; de Paz, M.V.; Valencia, C.; Franco, J.M. Synthesis and characterization of isocyanate-functionalized pva-based polymers with applications as new additives in lubricant formulations. *J. Appl. Polym. Sci.* **2012**, *125*, 3259–3267.
138. Gomez, I.; Otazo, E.M.; Prieto, F.; Guevara, A.; Villagomez, J.R. Experimental design of the microwave assisted synthesis of the poly(vinyl phenylthionecarbamate). *Tetrahedron Lett.* **2013**, *54*, 4285–4288.
139. Wang, J.; Ye, L. Structure and properties of hydrophobic cationic poly(vinyl alcohol). *Polym. Int.* **2012**, *61*, 571–580.
140. Fernández, M.D.; Fernández, M.J.; Hoces, P. Poly(vinyl acetal)s containing electron-donor groups: Synthesis in homogeneous phase and their thermal properties. *React. Funct. Polym.* **2008**, *68*, 39–56.
141. Delattre, E.; Lemièrre, G.; Desmurs, J.-R.; Boulay, B.; Duñach, E. Poly(vinyl alcohol) functionalization with aldehydes in organic solvents: Shining properties of poly(vinyl acetals). *J. Appl. Polym. Sci.* **2014**, *131*(17), 40677. doi:10.1002/APP.40677
142. Tong, Y.-Y.; Wang, R.; Xu, N.; Du, F.-S.; Li, Z.-C. Synthesis of well-defined azide-terminated poly(vinyl alcohol) and their subsequent modification via click chemistry. *J. Polym. Sci., Part A: Polym. Chem.* **2009**, *47*, 4494–4504.
143. Lee, E.; Park, J.; Im, S.G.; Song, C. Synthesis of single-walled carbon nanotube-incorporated polymer hydrogels via click chemistry. *Polym. Chem.* **2012**, *3*, 2451–2455.
144. Koohmareh, G.A.; Hajian, M.; Fallahi, H. Graft copolymerization of styrene from poly(vinyl alcohol) via raft process. *Intern. J. Polym. Sci.* **2011**, *2011*, 1–7. doi:10.1155/2011/190349
145. Onyar, J.M.; Huang, S.J. Synthesis and properties of novel poly(vinyl alcohol)-lactic acid gels. *J. Appl. Polym. Sci.* **2009**, *113*, 2053–2061.
146. Ding, J.; Chen, S.-C.; Wang, X.-L.; Wang, Y.-Z. Synthesis and properties of thermoplastic poly(vinyl alcohol)-*graft*-lactic acid copolymers. *Ind. Eng. Chem. Res.* **2009**, *48*, 788–793.
147. Ding, J.; Chen, S.-C.; Wang, X.-L.; Wang, Y.-Z. Preparation and rheological behaviors of thermoplastic poly(vinyl alcohol) modified by lactic acid. *Ind. Eng. Chem. Res.* **2011**, *50*, 9123–9130.
148. Silva, R.; Muniz, E.C.; Rubira, A.F. Multiple hydrophilic polymer ultra-thin layers covalently anchored to polyethylene films. *Polymer* **2008**, *49*, 4066–4075.
149. Lee, J.-H.; Lee, U.-S.; Jeong, K.-U.; Seo, Y.-A.; Park, S.-J.; Kim, H.-Y. Preparation and characterization of poly(vinyl alcohol) nanofiber mats crosslinked with blocked isocyanate prepolymer. *Polym. Int.* **2010**, *59*, 1683–1689.